Economic MPC of Wastewater Treatment Plants: Distributed Computing and Model Reduction

by

An Zhang

A thesis submitted in partial fulfillment of the requirements for the degree of

Master of Science

in

Process Control

Department of Chemical and Materials Engineering
University of Alberta

Abstract

Wastewater treatment plays an important role in the sustainable development of our society. A wastewater treatment plant (WWTP) is typically a large-scale nonlinear process composed of several interconnected operating units. To meet the strict environmental regulations, to ensure the operation safety and to reduce the operating cost, it is highly desired to monitor and operate WWTPs effectively. However, significant variations in the inlet flow rate and wastewater compositions have made the monitoring and control of WWTPs a very challenging task. Centralized economic model predictive control (EMPC) approach has been proposed to improve the control performance based on the economic considerations. However, the high computational complexity caused by solving the associated EMPC optimization problem can render the online implementation of this method intractable. In recent years, the distributed framework has been considered to be a promising framework to improve the applicability of EMPC for large-scale processes. Model linearization and model order reduction are also widely used to reduce the computational complexity of complex control problems.

This thesis focuses on improving the computational efficiency of EMPC for WWTPs. Two distributed EMPC designs are presented in this thesis. In the first design, the centralized model is used in each subsystem EMPC controller design; and in the second design, a subsystem model is used in each subsystem EMPC design. The performance of these two distributed EMPC designs are compared with a centralized model predictive control (MPC) scheme and a centralized EMPC scheme from different aspects including effluent quality, operating cost, and computational efficiency. It is found through vast simulations that the distributed EMPC with subsystem controller designed based on the entire system model is more favorable in terms of control performance.

Model reduction methods are also applied to the WWTP process in this thesis. In particular, the trajectory piecewise linear model and the order reduced trajectory piecewise linear model are used to approximate the original nonlinear system model. Two EMPC designs are proposed based on the two models. The approximated model accuracy are compared with the original nonlinear model. The performance of these two EMPC designs are compared with the EMPC based on the nonlinear model from control performance and computational efficiency points of view. We also investigate how the number of linearization points affect the EMPC control performance and computational efficiency through these applications. It is shown that there is a trade-off between the control performance and computational efficiency. The EMPC design based on the order reduced trajectory piecewise linear (TPWL-POD) model is more favorable since it significantly reduces the computational cost although degrades the control performance slightly.

Preface

The materials presented in this thesis are part of the research project under the supervision of Dr. Jinfeng Liu.

Chapter 3 of this thesis is a revised version of A. Zhang, X. Yin, S. Liu, J. Zeng and J. Liu. Distributed economic model predictive control of wastewater treatment plants. *Chemical Engineering Research and Design*, 141:144-155, 2019. I was responsible for the distributed EMPC design, simulations as well as the manuscript composition under the supervision of Professor Jinfeng Liu. X. Yin and S. Liu collaborated with me on the distributed EMPC design and contributed to manuscript edits. J. Zeng contributed to the model formulation for the wastewater treatment plants.

The Economic MPC design based on model reduction methods in Chapter 4 and the simulations for the design are my original work.

Acknowledgements

First and foremost, I would like to thank my supervisor Dr. Jinfeng Liu. I knew Jinfeng when I was taking my undergraduate course CHE 358 and CHE 573. I started to do research work with him since then. He is so nice and patient. He encouraged me a lot when I doubted myself. Without his continuous guidance and support, hardly can I finish my research work.

I would also like to thank my colleagues in the CPC group: Su Liu, Xunyuan Yin, Benjamin Decardi-Nelson, Guoyang Yan, Jannatan Nahar, Song Bo, Soumya Sahoo, Rui Nian, Bernard Twum Agyeman, Jianbang Liu, Yi Zhang and others. Su and Xunyuan helped me a lot during my graduate life and taught me a lot of fundamental knowledge about the process control theory. Whenever I met difficulties on the programming, Ben was the first one I came to ask for help. He checked my code, again and again, to help me solve problems. It was my great pleasure to work with them.

Nevertheless, I wish to give thanks to my friends who make my graduate life so wonderful. They are: Aijing Wang, Xinyao Zhu, Faye Zhou, Frane Sun and Zhuo-qun Shen. I would also thank my boyfriend Wenda Wang for his companion and continuous encouragement.

Finally, I must express my deepest gratitude to my parents for their unconditional love and unfailing support throughout my years of study. This accomplishment would not have been possible without them.

Contents

List of Tables

List of Figures

Chapter 1

Introduction

1.1 Motivation

Wastewater treatment plants (WWTPs) have been widely used to recycle wastewater in order to minimize its adverse environmental impacts. A typical WWTP is a large-scale nonlinear process consisted of a series of interconnected biological reactors and a secondary settler. While meeting the strict requirements in environmental regulations, ensuring the process safety and minimizing the cost of operation, a wastewater treatment plant should be well monitored and regulated [1]. However, significant variability of inlet flow rates and wastewater compositions leads to the increased complexity in the design of advanced control and monitoring schemes for WWTPs [2].

In the past decades, several control approaches have been proposed for WWTPs. In [3], proportional-integral (PI) controllers were designed for a nutrient removal WWTP operated under different control modes. In [4], PI controllers were designed to meet the effluent concentration criterion for WWTP. In [5], two tuning methods of PID controllers were proposed for the control of dissolved oxygen concentration in the activated sludge process. Although the PI controllers can be easily implemented, they cannot handle complex constraints or optimality considerations. To address these limitations, model predictive control (MPC) has attracted much research attention during the past decades. MPC predicts the future behaviour of the plant and

optimizes the control performance based on an explicit model [6]. At each control interval, the trajectories of future manipulated control inputs are generated by solving a finite horizon optimal control problem [7]. In [8–10], simultaneous design and control methods for wastewater treatment process were proposed based on MPC. In [11], a multi-variable feedback MPC controller was proposed for the Benchmark Simulation Model No.1 (BSM1), and the tuning of this MPC was discussed. MPC schemes were used to control the oxygen concentration in [12] and [13]. In [14] and [15], set-point tracking MPC was applied to a WWTP to increase the plant efficiency, and in [16] it was applied to reduce the power usage as well. While set-point tracking MPC can force concerned states towards the desired set-point, it does not explicitly consider the associated operating cost. As a result, the set-point operation of these existing methods may lead to increased operating cost. An alternative way to address the regulation of WWTP is to use economic MPC (EMPC). By using a more general cost function, EMPC is capable of handling the economic considerations explicitly. In [17], a centralized EMPC approach was proposed to improve the effluent quality and to minimize the overall operating cost. It is worth mentioning that the high computational complexity caused by solving the associated optimization problem can render the online implementation of this method intractable. Also, the relatively poor fault tolerance of a centralized control system is yet another factor that hinders its implementation.

To improve the applicability of the EMPC for large-scale processes, a natural consideration is to employ a distributed framework. A typical distributed control method divides a large problem into smaller sub-problems such that the evaluation of each controller can be made much less computationally demanding. Each local controller evaluates the optimal control input trajectories based both on local information and information exchanged with other controllers. The use of a distributed framework can also lead to improved fault tolerance, maintenance flexibility as well as computational efficiency [18–23]. Reviews and methods on distributed control based on model predic-

tive control can be found in [18–21, 24–27]. During the past several years, distributed EMPC has become a heated research topic. In [28], a distributed EMPC method was introduced for alkylation of benzene process network. The EMPC controller was also applied in a distributed scheme for nonlinear systems in [29]. In [30], a distributed EMPC strategy was applied to a catalytic reaction process, and a Lyapunov-based distributed EMPC with safety considerations was proposed for this process in [31]. In [32], a distributed economic MPC scheme was implemented for cooperative control of self-interested systems.

Applying a linear approximated model to the original nonlinear system is another way to improve the computational efficiency of EMPC for large-scale processes. A lot of achievements have been made on the use of approximated models in MPC. The work of [33] applied feedback linearization to the plant and then used MPC in a cascade arrangement for the resulting linear system. The nonlinear programming problem is reduced to a quadratic optimization problem which can improve the computational efficiency. The implementation of MPC with a different linear model at each time step derived from a local (Jacobian) linearization of the nonlinear plant was first proposed in [34]. Extended Kalman filter was proposed to be added to this approach to deal with the unstable nonlinear process and ensure a better disturbance rejection in [35] and [36]. This idea is further developed in [37], contraction constraints were applied and the explicit stability conditions were derived. In [38], one technique was proposed to approximate the nonlinear system with a linear time varying (LTV) model, which is obtained from a linearization of the system along the predicted system trajectory. In [39] and [40], a novel MPC algorithm was proposed which can significantly reduce the online computational demand. The approach is to only compute the first control move while approximating the rest of control moves by using a linear controller.

Model order reduction techniques can significantly abate the complexity of the nonlinear system while conserve the dominant dynamics of the process [41]. The

proper orthogonal decomposition (POD) method is extensively used in data analysis for approximating the high-dimensional process by low-dimensional descriptions [42]. The POD method has been widely applied in control in chemical engineering [43–47]. In [48], a state estimation scheme was established for WWTPs using POD-based model approximation. In [49] and [50] a reduced order model based on the POD-Galerkin projection method is constructed for economic MPC. With the reduced order model, the computational time is significantly reduced. In [51], a nonlinear system is represented by a piecewise-linear system and each of the pieces are reduced with a Krylov projections.

Motivated by the success of distributed EMPC and model reduction in different applications, in this thesis, we first apply distributed EMPC to WWTPs to address the computational complexity of a centralized EMPC. At the same time, we investigate through this application a few issues that have not been well addressed in the distributed EMPC literature: (a) how to decompose subsystems for distributed EMPC, (b) how the model used in each individual controller may affect the performance of the distributed EMPC. We also apply the trajectory piecewise linearization and a combination of trajectory piecewise linearization and proper orthogonal decomposition method to WWTPs to derive low-order linear model, which are subsequently used for EMPC controller design. The model accuracy, computational time, and economic control performance of the WWTP process under these EMPC controllers are compared in this thesis.

1.2   Thesis outline and contributions

The outline of the thesis and the contributions of each chapter are described as follows:

Chapter 2 is a preliminary chapter which provides the description of the notations and terms used in this thesis. The detailed wastewater treatment plant model used in the thesis is also described in this chapter.

In Chapter 3, the description of the WWTP process and its performance indices

4

are provided. The decomposition of the WWTP for distributed control is presented. Two different distributed EMPC are designed and the performance of these controllers is compared under dry, rainy and stormy weather conditions.

In Chapter 4, a modified WWTP process model is introduced. The trajectory piecewise linearization methodology and order reduced trajectory piecewise linearization method are presented. Two EMPC controllers are designed based on these models. The control performance and computation efficiency of these controllers are compared in dry weather condition.

The last chapter, Chapter 5 provides the summary on the results of this thesis and discusses the potential directions for future research work.

Chapter 2

Preliminaries

2.1 Terms and Definitions

Some of the key terms used throughout this thesis are listed and explained in this section.

- **WWTP**: wastewater treatment plant

- **BSM1**: benchmark simulation model No.1

- **ASM1**: activated sludge model No.1

- **EQ**: effluent quality

- **OCI**: operating cost index

- **MPC**: model predictive control

- **EMPC**: economic model predictive control

- **DEMPC**: distributed economic model predictive control

- **DEMPCS**: DEMPC based on subsystem model

- **DEMPCE**: DEMPC based on entire system model

- **TPWL**: trajectory piecewise linearization
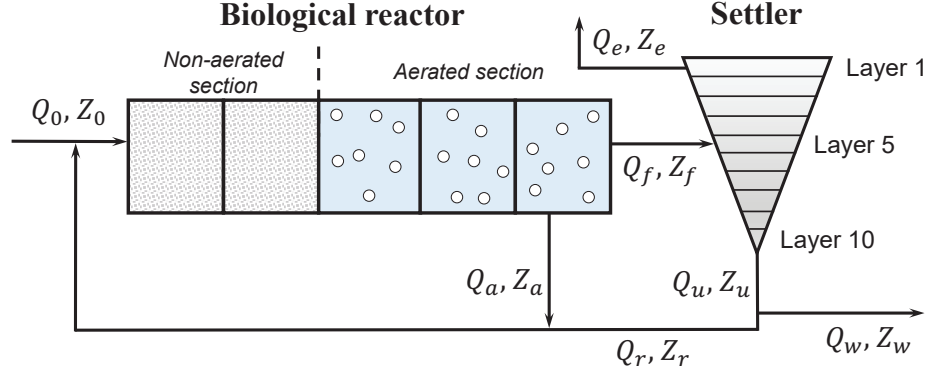
Figure 2.1: A schematic of the wastewater treatment plant

- **POD**: proper orthogonal decomposition

- **SVD**: singular value decomposition

- **TPWL-POD**: order reduced TPWL using POD method

In this thesis, the **plant** or **entire system** or **nonlinear system** means the whole system, while the **subsystem** indicates the distributed operating units that have their own controllers. **Local** is used to indicate the objects which belong to subsystems, such as **local controller**, **local subsystem model**, etc. A **local controller** refers to the local EMPC in a subsystem in the distributed control network. **Centralized EMPC** refers to the entire system is controlled by one controller.

2.2 WWTP description and modeling

2.2.1 Model description

A schematic diagram of a WWTP based on the BSM1 is presented in Figure 2.1 [2]. The process comprises a multi-chamber biological activated sludge reactor and a secondary settler. The biological reactor has two sections: the non-aerated section containing the first two anoxic chambers and the aerated section consisting of the remaining three chambers. In particular, pre-denitrification reactions where nitrate is turned into nitrogen by using bacteria and oxygen attached to nitrate ions take place

Table 2.1: Definition and notation of the process variables of the WWTPs

Definition	Notation	Unit
inert soluble organic matter	S_I	$g\ COD \cdot m^{-3}$
inert particulate organic matter	X_I	$g\ COD \cdot m^{-3}$
readily biodegradable and soluble substrate	S_s	$g\ COD \cdot m^{-3}$
slowly biodegradable and soluble substrate	X_s	$g\ COD \cdot m^{-3}$
biomass of active autotrophs	X_{B_A}	$g\ COD \cdot m^{-3}$
biomass of active heterotrophs	X_{B_H}	$g\ COD \cdot m^{-3}$
particulate generated from decay of organisms	X_P	$g\ COD \cdot m^{-3}$
particulate biodegradable organic nitrogen	X_{ND}	$g\ N \cdot m^{-3}$
nitrite nitrogen and nitrate	S_{NO}	$g\ N \cdot m^{-3}$
free and saline ammonia	S_{NH}	$g\ N \cdot m^{-3}$
biodegradable and soluble organic nitrogen	S_{ND}	$g\ N \cdot m^{-3}$
dissolved oxygen	S_O	$g\ (\text{-}COD) \cdot m^{-3}$
alkalinity	S_{ALK}	$mol \cdot m^{-3}$
total sludge concentration in settler	X	$g\ COD \cdot m^{-3}$

in the non-aerated section, while nitrification processes during which ammonium is oxidized into nitrate by using bacteria occur in the aerated section. Eight processes of the biological behaviour taking place in the reactor [2]. The Activated Sludge Model No.1 (ASM1) is used to describe the biological phenomena taking place in the biological reactor [52].

In the process, wastewater enters the first chamber of the biological reactor at flow rate Q_0 and concentration Z_0. A portion of the effluent of the last aerobic chamber is recycled back (inner recycle) to the first chamber at flow rate Q_a and concentration Z_a, while the rest is fed into the settler at flow rate Q_f and concentration Z_f. The settler comprises 10 nonreactive layers, the 6-th layer of which is the feed layer. The outlets of the settler are made up of three parts: (a) the overflow of the settler which contains purified water removed continuously through the first layer at flow rate Q_e; (b) a portion of the underflow of the settler fed back into the first chamber (outer

recycle) at flow rate Q_r; (c) the remaining portion of the underflow discharged from the settler at flow rate Q_w. In this model, eight basic biological reaction processes are considered, and 13 major compounds involved in these reactions are taken into account. The concentrations of the 13 compounds in the five chambers constitute the state variables of the model of the biological reactor. We present the definitions of the 13 state variables for each chamber in Table 2.1.

In the work, two manipulated inputs are taken into account, i.e., the flow rate of the recirculation stream (i.e., Q_a) and the oxygen transfer rate in the fifth chamber of the reactor (i.e., $K_L a_5$).

A more detailed description of the process model and the process parameters are reported in following subsection [2].

2.2.2 Dynamic model of WWTP

The dynamics of the WWTP process based on BSM1 model can be described by a total of 145 ordinary differential equations. In particular, each of the reactor compartments can be described by 13 differential equations according to the first 13 state variables defined in Table 2.1, and the dynamics of each layer in the secondary settler can be described by 8 ordinary differential equations. The state variables considered in the secondary settler are: total sludge concentration X (i.e., a weighted summation of X_I, X_S, X_P, $X_{B,H}$ and $X_{B,A}$), S_I, S_S, S_{NO}, S_{NH}, S_{ND}, S_O, and S_O. The parameter values of this process model used in this thesis are presented in Table 2.2.

Dynamics of the biological reactors

The dynamics of the biological reactors are described based on mass balance as follows:

For compartment k ($k = 1$) of the biological reactor:

$$\frac{dZ_1}{dt} = \frac{1}{V_1}(Q_a Z_a + Q_r Z_r + Q_0 Z_0 + r_1 V_1 - Q_1 Z_1) \tag{2.1a}$$

$$Q_1 = Q_a + Q_r + Q_0 \tag{2.1b}$$

Table 2.2: Parameter value of the model

V_1 (volume of chamber 1)	1000 m^3
V_2 (volume of chamber 2)	1000 m^3
V_3 (volume of chamber 3)	1333 m^3
V_4 (volume of chamber 4)	1333 m^3
V_5 (volume of chamber 5)	1333 m^3
Q_w (Underflow discharge flow rate)	385 m^3/d
Q_r (Outer recycle flow rate)	18446 m^3/d
V_s (Volume of settler)	6000 m^3
A (Cross-sectional area of settler)	1500 m^2
$K_L a_3$ (Oxygen transfer coefficient of chamber 3)	240 d^{-1}
$K_L a_4$ (Oxygen transfer coefficient of chamber 4)	240 d^{-1}
H_s (Height of settler)	4 m
H_j $j = 1, \ldots, 10$ (Height of each layer)	0.4 m
N_{layer} (Number of layers)	10

For compartment k $(k = 2, \ldots, 5)$ of the biological reactor:

$$\frac{dZ_k}{dt} = \frac{1}{V_k}(Q_{k-1}Z_{k-1} + r_k V_k - Q_k Z_k) \tag{2.2a}$$

$$Q_k = Q_{k-1} \tag{2.2b}$$

Special case for concentration $S_{O,k}$, $k = 1, \ldots, 5$, (the concentration of dissolved oxygen in compartment k of the biological reactor):

$$\frac{dS_{O,k}}{dt} = \frac{1}{V_k}(Q_{k-1}S_{O,k-1} + r_k V_k + K_L a_k V_k(S_O^* - S_{O,k}) - Q_k S_{O,k}) \tag{2.3}$$

Some concentration and flowrate relationships inside the process:

$$Z_a = Z_5 \tag{2.4a}$$

$$Z_f = Z_5 \tag{2.4b}$$

$$Z_w = Z_r \tag{2.4c}$$

$$Q_f = Q_5 - Q_a = Qe + Q_r + Q_w = Q_e + Q_u \tag{2.4d}$$

In Eq. (2.1), Eq. (2.2), Eq. (2.3), and Eq. (2.4), Z_k is the concentration of the compounds defined in Table 2.1 in kth compartment of the biological reactor, V_k represents the volume of kth compartment, S_O^* is the saturation concentration for oxygen and is equal to 8 g.m^{-3}, and K_La_k represents the oxygen transfer coefficient in kth compartment, since compartments 1 and 2 of the reactor are anoxic compartments, $K_La_1 = K_La_2 = 0$ d^{-1} [2].

In Eq. (2.1), Eq. (2.2), and Eq. (2.3), r_k denotes the observed conversion rates of the compound in kth compartment, and it can be expressed as follows:

- S_I $(i = 1)$:

$$r_1 = 0 \tag{2.5}$$

- S_S $(i = 2)$:

$$r_2 = -\frac{1}{Y_H}\rho_1 - \frac{1}{Y_H}\rho_2 + \rho_7 \tag{2.6}$$

- X_I $(i = 3)$:

$$r_3 = 0 \tag{2.7}$$

- X_S $(i = 4)$:

$$r_4 = (1 - f_p)\rho_4 + (1 - f_p)\rho_5 - \rho_7 \tag{2.8}$$

- $X_{B,H}$ $(i = 5)$:

$$r_5 = \rho_1 + \rho_2 - \rho_4 \tag{2.9}$$

- $X_{B,A}$ $(i = 6)$:

$$r_6 = \rho_3 - \rho_5 \tag{2.10}$$

- X_P ($i = 7$):

$$r_7 = f_P \rho_4 + f_P \rho_5 \tag{2.11}$$

- S_O ($i = 8$):

$$r_8 = -\frac{1 - Y_H}{Y_H} \rho_1 - \frac{4.57 - Y_A}{Y_A} \rho_3 \tag{2.12}$$

- S_{NO} ($i = 9$):

$$r_9 = -\frac{1 - Y_H}{2.86 Y_H} \rho_2 + \frac{1}{Y_A} \rho_3 \tag{2.13}$$

- S_{NH} ($i = 10$):

$$r_{10} = -r_{XB} \rho_1 - i_{XB} \rho_2 - (i_{XB} + \frac{1}{Y_A}) \rho_3 + \rho_6 \tag{2.14}$$

- S_{ND} ($i = 11$):

$$r_{11} = \rho_{11} - \rho_6 + \rho_8 \tag{2.15}$$

- X_{ND} ($i = 12$):

$$r_{12} = (i_{XB} - f_P i_{XP}) \rho_4 + (i_{XB} - f_P i_{XP}) \rho_5 - \rho_8 \tag{2.16}$$

- S_{ALK} ($i = 13$):

$$r_{13} = -\frac{i_{XB}}{14} \rho_1 + (\frac{1 - Y_H}{14 \times 2.86 Y_H} - \frac{i_{XB}}{14} + \frac{1}{7 Y_A}) \rho_3 + \frac{1}{14} \rho_6 \tag{2.17}$$

where ρ_k, $k = 1$ to 8, stands for the eight biological processes of the system, and it can be shown as follows:

- Aerobic growth of heterotrophic biomass $X_{B,H}$:

$$\rho_1 = \mu_H (\frac{S_S}{K_S + S_S})(\frac{S_O}{K_{O,H} + S_O}) X_{B,H} \tag{2.18}$$

12

- Anoxic growth of heterotrophic biomass (denitrification):

$$\rho_2 = \mu_H\left(\frac{S_S}{K_S + S_S}\right)\left(\frac{K_{O,H}}{K_{O,H} + S_O}\right)\left(\frac{SNO}{KNO + S_{NO}}\right)\eta_g X_{B,H} \qquad (2.19)$$

- Aerobic growth of autotrophic biomass $X_{B,A}$ (nitrification):

$$\rho_3 = \mu_A\left(\frac{S_{NH}}{K_{NH} + S_{NH}}\right)\left(\frac{S_O}{K_{O,A} + S_O}\right)X_{B,A} \qquad (2.20)$$

- Decay of heterotrophic biomass:

$$\rho_4 = b_H X_{B,H} \qquad (2.21)$$

- Decay of autotrophic biomass:

$$\rho_5 = b_A X_{B,A} \qquad (2.22)$$

- Ammonification of soluble organic nitrogen:

$$\rho_6 = k_a S_{ND} X_{B,H} \qquad (2.23)$$

- Hydrolysis of entrapped organics:

$$\rho_7 = k_h \frac{X_S/X_{B,H}}{K_X + (X_S/X_{B,H})}\left[\left(\frac{S_O}{K_{O,H} + S_O}\right) + \eta_h\left(\frac{K_{O,H}}{K_{O,H} + S_O}\right)\left(\frac{S_{NO}}{K_{NO} + S_{NO}}\right)\right] X_{B,H}$$
$$(2.24)$$

- Hydrolysis of entrapped organic nitrogen:

$$\rho_8 = k_h \frac{X_S/X_{B,H}}{K_X + (X_S/X_{B,H})}\left[\left(\frac{S_O}{K_{O,H} + S_O}\right)\left(\frac{S_{NO}}{K_{NO} + S_{NO}}\right)\right] X_{B,H}(X_{ND}/X_S)$$
$$(2.25)$$

Table 2.3 presents the stoichiometric parameter values and Table 2.4 shows the kinetic parameter values used in the above biological process expressions. The biological parameter values shown bellow correspond approximately to a temperature of 15 °C.

Table 2.3: Stoichiometric parameter values

Parameter	Unit	Value
Y_A	g cell COD formed (g N oxidized)$^{-1}$	0.24
Y_H	g cell COD formed (g COD oxidized)$^{-1}$	0.67
f_P	dimensionless	0.08
i_{XB}	g N (g COD)$^{-1}$ in biomass	0.08
i_{XP}	g N (g COD)$^{-1}$ in particular products	0.06

Table 2.4: Kinetic parameter values

Parameter	Unit	Value
μ_H	d^{-1}	4.0
K_S	g COD m$^-3$	10.0
$K_{O,H}$	g (-COD) m$^-3$	0.2
K_{NO}	g NO$_3$-N m$^-3$	0.5
b_H	d^{-1}	0.3
η_g	dimensionless	0.8
η_h	dimensionless	0.8
k_h	g slowly biodegradable COD (g COD d)$^{-1}$	3.0
K_X	g slowly biodegradable COD (g COD)$^{-1}$	0.1
μ_a	d^{-1}	0.5
K_{NH}	g NH$_3$-Nm^{-3}	1.0
b_A	d^{-1}	0.05
$K_{O,A}$	g (-COD)m^{-3}	0.4
k_a	m^3(g COD d)$^{-1}$	0.05

Dynamics of the secondary settler

The model for the secondary settler is established based on the assumption that the dynamics of the particulate concentrations of the inlet to the settler can immediately diffuse to the top and the bottom layers of the settler; that is, the sludge retention time in the settler is neglected. The dynamics of the settler is modeled based on mass balances of the sludge considering solid flux due to gravity [53].

The dynamics of the sludge based on mass balance can be shown as follows:

For the bottom layer $m = 1$:

$$\frac{dX_1}{dt} = \frac{\nu_{dn}(X_2 - X_1) + \min(J_{s,2}, J_{s,1})}{z_1} \tag{2.26}$$

For layers $m = 2$ to $m = 5$:

$$\frac{dX_m}{dt} = \frac{\nu_{dn}(X_{m+1} - X_m) + \min(J_{s,m}, J_{s,m+1}) - \min(J_{s,m}, J_{s,m-1})}{z_m} \tag{2.27}$$

For the feed layer $m = 6$:

$$\frac{dX_6}{dt} = \frac{(Q_f X_f)/A + J_{clar,7} - (\nu_{up} - \nu_{dn})X_m - \min(J_{s,m}, J_{s,m-1})}{z_m} \tag{2.28}$$

For layers $m = 7$ to $m = 9$:

$$\frac{dX_m}{dt} = \frac{\nu_{up}(X_{m-1} - X_m) + J_{clar,m+1} - J_{clar,m}}{z_m} \tag{2.29}$$

For the top layer $m = 10$:

$$\frac{dX_{10}}{dt} = \frac{\nu_{up}(X_9 - X_{10}) - J_{clar,10}}{z_{10}} \tag{2.30}$$

In the above equations, the term $J_{clar,j}$ $(j = 1$ to $7)$ is assumed to be:

$$J_{clar,j} = \nu_{s,j} X_j \tag{2.31}$$

The solid flux due to gravity (J_s) can be calculated as:

$$J_s = \nu_s(X) X \tag{2.32}$$

where X is the total sludge concentration.

The settling velocity $\nu_s(X)$ is computed based on a double-exponential settling velocity function as follows [53]:

$$\nu_s(X) = \nu_0(e^{-r_h(X - X_{min})} - e^{-r_p(X - X_{min})} \tag{2.33}$$

$$X_{min} = f_{ns} X_f \tag{2.34}$$

In the settling velocity function Eq. (2.33), the value for parameters ν_0, r_h, r_p, and f_{ns} are equal to 474, 0.000576, 0.00286, and 0.00228, respectively. The term X_f is calculated as follows:

$$X_f = 0.75(X_{S,5} + X_{P,5} + X_{I,5} + X_{B,H,5} + X_{B,A,5}) \tag{2.35}$$

The dynamics for the soluble components (including dissolved oxygen) can be shown as follows:

For layers $m = 1$ to $m = 5$:

$$\frac{dZ_m}{dt} = \frac{\nu_{dn}(Z_{m+1} - Z_m)}{z_m} \tag{2.36}$$

For the feed layer $m = 6$:

$$\frac{dZ_6}{dt} = \frac{(Q_f Z_f)/A - (\nu_{dn} + \nu_{up})Z_6}{z_6} \tag{2.37}$$

For layers $m = 7$ to $m = 10$:

$$\frac{dZ_m}{dt} = \frac{\nu_{up}(Z_{m+1} - Z_m)}{z_m} \tag{2.38}$$

In the above eqeuations Eq. (2.26) to Eq. (2.38), ν_{dn} and ν_{up} are defined as follows:

$$\nu_{dn} = \frac{Q_u}{A} = \frac{Q_r + Q_w}{A} \tag{2.39}$$

$$\nu_{up} = \frac{Q_e}{A} \tag{2.40}$$

2.3   Conclusions

In this chapter, the definitions of the notations and terms used in this thesis are given, and a detailed wastewater treatment plant model used in this thesis is introduced. The introduced BSM1 model is used as the process model in Chapter 3, and a modified BSM1 model is used as the process model in Chapter 4.

Chapter 3

Distributed economic model predictive control of wastewater treatment plants [1]

3.1 Introduction

In this chapter, we apply distributed EMPC to a WWTP described by BSM1. After the description of the WWTP process and its performance indices, we consider the decomposition of the WWTP for distributed control which is the basis of a successful distributed design [56, 59, 61, 62]. The entire plant is decomposed into two subsystems for distributed EMPC design. The decomposition takes into account both the topology of the process and the need in distributed control system design as well as computational consideration. Based on the decomposed subsystems, we design distributed EMPC. For each subsystem, a local EMPC is designed. We consider two different distributed EMPC designs. In one design, the entire centralized plant model is used in each local controller; in the other case, each subsystem EMPC is designed based on the corresponding local subsystem model. The control objective of each local controller is to minimize the economic control cost, and the economic control cost function is determined as a weighted summation of the effluent quality (EQ) and the operating cost index (OCI). The computational efficiency of the two

---

[1]This chapter is a revised version of "A. Zhang, X. Yin, S. Liu, J. Zeng, and J. Liu, Distributed economic model predictive control of wastewater treatment plants. Chemical Engineering Research and Design, 141:144-155, 2019"

distributed EMPC designs is also investigated and compared with centralized EMPC. It is found through extensive simulations that the distributed EMPC with subsystem controller designed based on the entire system model is more favorable in terms of control performance.

3.2 Preliminaries

3.2.1 Compact form of the system model

The BSM1 model for the wastewater treatment plants can be written in the following compact form:

$$\dot{x}(t) = f\left(x(t), u(t), p(t)\right) \tag{3.1}$$

where $x \in \mathbb{R}^{145}$ is the state vector of the process, $u = [u_1 \ u_2]^T = [Q_a \ K_L a_5]^T \in \mathbb{R}^2$ is the input vector containing the two manipulated inputs, and $p \in \mathbb{R}^{14}$ is the known input vector containing the influent information of inlet flowrate Q_0 and concentration Z_0. The system states and inputs satisfy the following constraints: $x \in \mathbb{X}$, and $u \in \mathbb{U}$, where $\mathbb{X}$ and $\mathbb{U}$ are compact sets.

3.2.2 Performance evaluation criteria

The quality of the settler effluent and the overall operating cost are two essential features for performance assessment of a WWTP. The two features can be quantitatively assessed by two performance indices, i.e., the effluent quality (EQ) which is obtained by calculating the average amount of the pollutants discharged, and the overall cost index (OCI) which incorporates the factors that substantially contribute to the operating costs. The two indices are also important for evaluating the performance of different control schemes. In the following, the concepts of EQ and OCI are introduced in detail.

Table 3.1: Values of the weighting coefficients of EQ Index

Weighting coefficient	β_{SS}	β_{COD}	β_{NKj}	β_{NO}	β_{BOD}	f_p	i_{XB}	i_{XP}
Value	2	1	30	10	2	0.08	0.08	0.06

Effluent quality

In BSM1, EQ (kg pollution unit $\cdot$ day^{-1}) represents the daily average of a weighted summation of the effluent concentrations of several compounds, which significantly affect the quality of the processed water according to regional regulations. Specifically, the EQ index is evaluated as follows:

$$
\text{EQ} = \frac{1}{T \cdot 1000} \int_{t_0}^{t_f} \left(\begin{array}{c} \beta_{\text{SS}} \cdot \text{SS}_e(t) + \beta_{\text{COD}} \cdot \text{COD}_e(t) + \beta_{NKj} \cdot S_{NKj,e}(t) \\ + \beta_{NO} \cdot S_{NO,e}(t) + \beta_{\text{BOD}} \cdot \text{BOD}_e(t) \end{array} \right) Q_e(t)dt
$$

(3.2)

where

$$
\text{SS}_e = 0.75 \left(X_{S,e} + X_{B_A,e} + X_{B_H,e} + X_{I,e} + X_{P,e} \right)
$$

$$
\text{COD}_e = S_{I,e} + S_{S,e} + X_{S,e} + X_{I,e} + X_{B_H,e} + X_{B_A,e} + X_{P,e}
$$

$$
\text{BDO}_e = 0.25 \left(S_{S,e} + X_{S,e} + (1 - f_p) \left(X_{B_A,e} + X_{B_H,e} \right) \right)
$$

$$
S_{NKj,e} = S_{ND,e} + S_{NH,e} + X_{ND,e} + i_{XB} \left(X_{B_A,e} + X_{B_H,e} \right) + i_{XP} \left(X_{I,e} + X_{P,e} \right)
$$

In Eq. (3.2), t_0 and t_f denote the initial and final time instants of the evaluation horizon; $T := t_f - t_0$ is the length of the horizon, and is usually selected to be $T = 7$ days; SS represents the concentration of suspended solids, COD is chemical oxygen demand, BOD denotes the biological oxygen demand, and S_{NKj} denotes the concentration of Kjeldahl nitrogen; β_{SS}, β_{COD} β_{NKj}, β_{NO} and β_{BOD} represent the weighting coefficients used to calculate EQ; f_p, i_{XB}, and i_{XP} are stoichiometirc parameters. The corresponding values are listed in Table 3.1 [54] and the subscript "e" refers to the effluent of the secondary settler.

Overall cost index

The total operating cost required for processing wastewater is another important factor in performance evaluation. Factors that have major effects on the operating cost include the sludge production that needs to be disposed, the energy required for aerating and pumping, external carbon consumption as well as mixing energy.

The sludge production (SP) is defined as the average amount per day $(\text{kg} \cdot \text{day}^{-1})$ of the solids produced in the process over the evaluation horizon T, including the solids discharged through the wastage flow Q_w from the settler and the sedimentary solids in a WWTP plant.

$$
\begin{aligned}
\text{SP} = & \frac{0.75}{T \cdot 1000} \int_{t_0}^{t_f} \left(X_{S,w}(t) + X_{I,w}(t) + X_{B_A,w}(t) + X_{B_H,w}(t) + X_{P,w}(t) \right) Q_w(t) dt \\
& + \frac{1}{T \cdot 1000} \left(\text{SS}(t_f) - \text{SS}(t_0) \right)
\end{aligned}
\tag{3.3}
$$

In Eq. (3.3), the subscript "w" refers to the wastage outlet of the secondary settler.

The aeration energy (AE) $(\text{kWh} \cdot \text{day}^{-1})$ is associated with several plant characteristics, including the diffuser type, the submersion depth, the bubble size, etc. AE is calculated based on the oxygen transfer rates (i.e., $K_L a_i$, $i = 1, \ldots, 5$) by considering an immersion depth of 4m as follows:

$$
\text{AE} = \frac{S_o^{sat}}{T \cdot 1800} \int_{t_0}^{t_f} \sum_{i=1}^{5} V_i \cdot K_L a_i(t) dt
\tag{3.4}
$$

where $\mathbb{I} := \{i | \ i \in \{1\ 2\ 3\ 4\ 5\}\}$, V_i denotes the volume of the i-th chamber of the sludge reactor, and $K_L a_i$ denotes the oxygen transfer rate in the i-th chamber. S_o^{sat} denotes the saturation concentration of oxygen and its value is 8g/m^3.

The pumping energy (PE) $(\text{kWh} \cdot \text{day}^{-1})$ represents the energy consumed by the pumps used for inner recycle (i.e., Q_a) and outer recycle (i.e., Q_r). PE is calculated as below:

$$
\text{PE} = \frac{1}{T} \int_{t_0}^{t_f} \left(0.004 Q_a(t) + 0.05 Q_w(t) + 0,008 Q_r(t) \right) dt
\tag{3.5}
$$

The mixing energy (ME) (kWh · day^{-1}) denotes the energy consumed for mixing the compounds in the anoxic chambers to avoid the occurrence of settling. ME is calculated depending on the volume of each chamber and the oxygen transfer rates:

$$\mathrm{ME} = \frac{24}{T} \int_{t_0}^{t_f} \left(\sum_{i \in \mathbb{I}} 0.005 \cdot V_i \right) dt \tag{3.6}$$

where $\mathbb{I} := \{i| \ i \in \{1 \ 2 \ 3 \ 4 \ 5\}\}$.

The overall cost index (OCI) approximates the total cost for WWTP operation by taking a weighted summation of the listed major factors as follows:

$$\mathrm{OCI} = 5 \cdot \mathrm{SP} + \mathrm{AE} + \mathrm{PE} + \mathrm{ME} \tag{3.7}$$

3.2.3 Economic control objective

The economic control objective for EMPC is defined as

$$l(x, u) = l_{\mathrm{eco}}(x, u) + \delta u \tag{3.8}$$

In Eq. (3.8), $l_{\mathrm{eco}}(x, u)$ is the economic index to be minimized in entire system and is defined as:

$$l_{\mathrm{eco}}\left(x(\tau), u(\tau)\right) = \left(\alpha_{\mathrm{EQ}} \widehat{\mathrm{EQ}}(\tau) + \alpha_{\mathrm{OCI}} \widehat{\mathrm{OCI}}(\tau) \right) \tag{3.9}$$

where $\widehat{\mathrm{EQ}}$ and $\widehat{\mathrm{OCI}}$ are the two economic index: EQ and OCI which are defined in Eq. (3.2) and Eq. (3.7) respectively. α_{EQ} and α_{OCI} are two weighting coefficient for effluent quality index and operating cost index.

In Eq. (3.8), δu is used to penalize the changing rate of input u and its description will be presented in the formulation of local EMPC design.

3.3 Subsystem decomposition of the WWTP

In this section, we aim at decomposing the WWTP into subsystems for distributed EMPC design.

3.3.1 Guidelines for subsystem decomposition

When performing subsystem decomposition, we follow three guidelines as below: (a) it is required to have at least one manipulated input variable in each configured subsystem; (b) it is expected that the subsystem decomposition result does not violate the process topology; (c) it is favorable to have similar numbers of state variables in the configured subsystems.

The considerations behind the guidelines are explained as follows. First, one distributed EMPC controller will be designed for each subsystem. Therefore, we require that each subsystem is assigned with at least one input such that each formulated subsystem EMPC has at least one decision variable selected from the available manipulated inputs. Second, it is better not to decompose the state variables from the same physical unit into different subsystems, or else the communication and maintenance complexity of the subsystem controller will be increased significantly. Third, the subsystem controllers are designed based on an EMPC algorithm, of which the computational complexity is non-negligible in implementation. Having similar numbers of state variables in the subsystems can help achieve balanced computational loads for the subsystem EMPC controllers.

3.3.2 Subsystem configuration results

Since there are only two manipulated inputs in the WWTP, the process is decomposed into two subsystems. One subsystem is assigned with input Q_a while the other subsystem is assigned with input K_La_5. Taking into account the process topology and the numbers of states in each physical unit, the two subsystems are configured as follow.

- Subsystem 1: Chamber 1 to Chamber 4

- Subsystem 2: Chamber 5 and the secondary settler

Within this configuration, we assign Q_a to the first subsystem as this input directly

affects the dynamics of the first chamber from a topological point of view. Similarly, K_La_5 is assigned to the second subsystem since this input is associated with the process through Chamber 5 which belongs to the second subsystem. The numbers of the states of the first subsystem and the second system are 52 and 93, respectively.

Remark 3.3.1 *It is possible to include one or more manipulated inputs, and use existing subsystem decomposition methods (e.g., [55, 56]) to decompose the process into three subsystems with more balanced scales. It is also possible to apply the decomposition methods [57–61] to obtain the optimal distributed control structure where the numbers of subsystem states may be made more similar. In [2] where the BSM1 model for the WWTP was originally reported, two variables (i.e., the flow rate of the recirculation stream denoted by Q_a and the oxygen transfer rate in the fifth chamber of the reactor denoted by K_La_5) are suggested as common manipulated inputs. In this chapter, we consider the two manipulated inputs and aim to design two local controllers accordingly. We would like to note that the computational complexity of the two local controllers is not vastly different, which will be shown through simulation results in Section 3.6.2.*

3.3.3 Subsystem model

The model of each decomposed subsystem of wastewater treatment plant can be described in the following form:

$$\dot{x}_i(t) = f_i(x_1(t), x_2(t), u_1(t), u_2(t), p(t)) \quad i = 1, \ 2 \tag{3.10}$$

where $x_1 \in \mathbb{R}^{52}$ and $x_2 \in \mathbb{R}^{93}$ are the states vectors of subsystem 1 and subsystem 2, respectively. $u_1 = Q_a$ is the manipulated input to subsystem 1 and $u_2 = K_La_5$ is the manipulated input to subsystem 2.
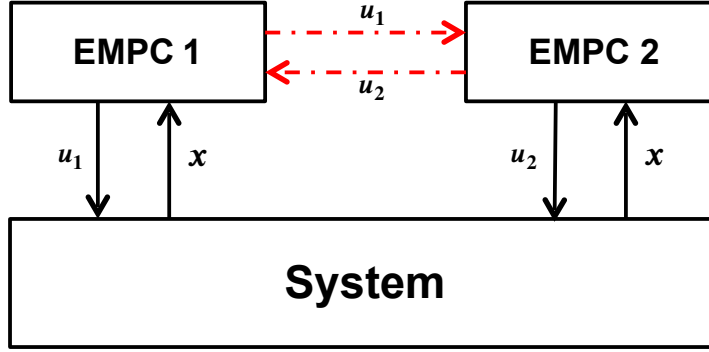
Figure 3.1: A diagram of the proposed DEMPC based on the entire system model

3.4 Distributed EMPC design based on the entire system model

Two different distributed EMPC (DEMPC) designs are considered. In the first design, the entire system model is used for local controller design; in the second design, the subsystem model is used. In this section, the distributed EMPC with each EMPC designed based on the entire system model for the WWTP is presented. The control objective is to minimize the economic control cost. Figure 3.1 shows a diagram of the DEMPC design based on the entire system model. During each sampling period, the two EMPC controllers receive state measurements from the plant and communicate with each other to exchange future manipulated inputs trajectories iteratively. The evaluation and communication protocol is supposed to satisfy the following requirements: (1) the two controllers are evaluated simultaneously and synchronously every sampling period; (2) at each sampling time $t_{k \geq 0}$, subsystem controller i, $i = 1,\ 2$, has access to the state measurement of the entire system $x(t_k)$ immediately; (3) The two controllers can exchange the latest future input trajectories immediately.

3.4.1 Implementation Strategy

The implementation strategy of the proposed iterative distributed EMPC design based on the entire system model for WWTPs is described by the following algorithm:

Algorithm 3.4.1 *Implementation algorithm for distributed EMPC based on the entire system model*

1. *At each sampling time $t_{k \geq 0}$, set $c = 1$, let the i-th EMPC controller receive entire system state measurements $x(t_k)$, let $u_i^{(0)}(\tau|t_k) = u_i^*(\tau|t_{k-1})$, $\tau \in [t_k, t_{k+N})$, where $u_i^*(\tau|t_{k-1})$ denotes the optimal input trajectory at instant t_{k-1}, and do the following steps:*

   1.1. *The i-th EMPC controller sends the future input trajectories generated from the previous iteration $c-1$ (i.e., $u_i^{(c-1)}(\tau|t_k)$, $\tau \in [t_k, t_{k+N})$, $i = 1, 2$) to the other controller.*

   1.2. *The i-th subsystem EMPC controller evaluates the future control input trajectory $u_i^{(c)}(\tau|t_k)$, $i = 1, 2$ based on the input trajectories from the previous iteration $u_j^{(c-1)}$, $j \neq i$.*

   1.3. ***If** $c = q$ **or** $|u_i^{(c)}(\tau|t_k) - u_i^{(c-1)}(\tau|t_k)| < \epsilon$, **then:***
   Let $u_i^* = u_i^{(c)}(\tau|t_k)$, and go to Step 2.
   ***Else**, do:*
   Set $c = c+1$, and go to Step 1.1.

2. *The i-th EMPC controller sends the first control input of the manipulated input $(u_i^*(t_k|t_k))$ to the actuator.*

In Algorithm 3.4.1, $c \geq 1$ denotes the number of iteration steps, and is bounded by q which is the maximum iteration steps. The value of q should be pre-determined. The termination condition for Algorithm 3.4.1 may also be improved such that the iteration ends either when it achieves the pre-set maximum iteration number q or when the difference in the calculated u in two consecutive iterations is small than the pre-set threshold value ϵ. At time instant t_0, each EMPC controller i, $i = 1, 2$, is initialized with steady-state values of the inputs of its interacting subsystems as a conservative approximation.

In Step 1, the optimal future input trajectory of the i-th EMPC controller at instant t_{k-1} is assumed as follow:

$$u_i^*(\tau|t_{k-1}) = u_i^*(t_{k+N-2}|t_{k-1}), \quad \tau \in [t_{k+N-1}, t_{k+N}) \tag{3.11}$$

Eq. (3.11) assumes that the optimal control input which is one sampling interval beyond the control horizon at t_{k-1} is the same as the last input within that control horizon in the first iteration evaluation of each sampling time.

3.4.2   Local EMPC design

The optimization problem for EMPC i, $i = 1, 2$, developed based on the entire system model at t_k in iteration c is formulated as follows:

$$u_i^{(c)}(\tau|t_k) = \arg \min_{u_i(\tau) \in S_i(\Delta)} \int_{t_k}^{t_{k+N}} l\left(\tilde{x}(\tau), u(\tau)\right) d\tau \tag{3.12a}$$

$$\text{s.t.} \quad \dot{\tilde{x}}(\tau) = f(\tilde{x}(\tau), u(\tau), p(\tau)) \tag{3.12b}$$

$$\tilde{x}(t_k) = x(t_k) \tag{3.12c}$$

$$u_j(\tau) = u_j^{(c-1)}(\tau), \quad j \neq i \tag{3.12d}$$

$$u_i(\tau) \in \mathbb{U}_i \tag{3.12e}$$

$$x(\tau) \in \mathbb{X} \tag{3.12f}$$

In the optimization problem Eq. (3.12), $u_i^{(c)}(\tau|t_k)$ denotes the optimal solution to this problem. Eq. (3.12a) is the objective function for the i-th EMPC controller where N is the control horizon, l is the global economic index being defined in Eq. (3.8), $S_i(\Delta)$ denotes a class of piecewise-constant functions, and $u(\tau)$ is equal to $[u_1(\tau) \ u_2(\tau)]^T$ for $\tau \in [t_k, t_{k+N})$. Eq. (3.12b) is the entire system model. In Eq. (3.12c), the predicted state trajectory is initialized with the state measurement at the current sampling time (i.e., $x(t_k)$) at each iteration. The future input trajectory in Eq. (3.12a) and Eq. (3.12b) is a concatenated vector of $u_i(\tau)$ and $u_j(\tau)$, and Eq. (3.12d) updates $u_j(\tau|t_k)$ with $u_j^{(c-1)}(\tau|t_k)$, $j \in \{1, 2\} \setminus \{i\}$, where $u_j^{(c-1)}(\tau|t_k)$ denotes the future input trajectory received from the other EMPC controller generated in previous iteration

26

step $c - 1$, and "\" denotes the set substraction. Eq. (3.12e) and Eq. (3.12f) impose constraints on the manipulated inputs and states to subsystem i, $i = 1, 2$.

In Eq. (3.8), the second term penalizes the rate of change of inputs, and is defined as follows:

$$\delta u(t) = |u(t) - u(t_{j-1})|^2_R, \quad t \in (t_{j-1}, t_j], \ j \in (k, k + N] \tag{3.13}$$

where R is the weighting coefficient for the changing rate of inputs.

Once the optimization problem in Eq. (3.12) is solved, a trajectory of u_i is obtained. The first step value is applied to the process; that is, the manipulated input applied to the system is with the following form:

$$u_i(t) = u_i^*(t|t_k), \ t \in [t_k, t_{k+1}), \ i = 1, 2 \tag{3.14}$$

Note that when $c = 1$, the future input sequence received from previous iteration step, $u_i^{(c-1)}(\tau|t_k)$, $\tau \in [t_k, t_{k+N})$, is set to be the optimal trajectory received at time instant t_{k-1}, $u_i^*(\tau|t_{k-1})$, $\tau \in [t_k, t_{k+N})$ with the input value $u_i^*(t|t_{k-1})$ for $t \in [t_{k+N-1}, \ t_{k+N})$ is defined in Eq. (3.11).

Remark 3.4.1 *Since the WWTP is a large-scale complex process with high nonlinearity, and its operation is subject to significant variations of the influent flow rates and compositions, it is highly possible that the optimal solution to each EMPC problem is not unique. The penalty on the rate of change of the inputs (which is defined in the Eq. (3.13)) can help avoid too significant fluctuation in the input sequence and achieve a unique solution when solving the optimization problem. The magnitude of the penalty and discussions on how the economic performance is affected by different values of the weight R are presented in Section 3.6.2.*

Remark 3.4.2 *Including a slack variable and imposing soft constraints on the rate of change of the input could be another promising way to design local controllers. In this chapter, we have not considered this type of designs. We choose to penalize the*
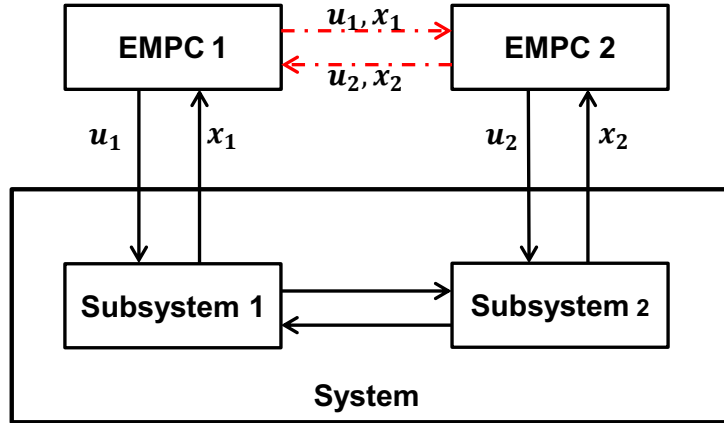
Figure 3.2: A diagram of the proposed DEMPC based on the subsystem model

rate of change of the control input in the objective function. If we introduce another slack variable and impose additional soft constraints on the rate of change of the inputs, the design of each local controller could be more conservative and the extent of the conservativeness depends on the constraints on the introduced slack variables. In future research, we may investigate this case, and compare the control performance between the two different designs.

3.5 DEMPC design based on the subsystem model

In this section, we discuss the proposed distributed EMPC with each local controller designed based on the subsystem model for the WWTP. A diagram of the proposed DEMPC scheme based on the subsystem model is given in Figure 3.2. An EMPC controller is developed for each subsystem. The two EMPC controllers exchange information in terms of manipulated inputs, subsystem state measurements and predicted future states with each other iteratively, and communicate with WWTP to receive the state measurements at the beginning of each time instant. The evaluation and communication protocol satisfies similar requirements as described in Section 3.4.

3.5.1 Implementation strategy

An implementation algorithm for the proposed distributed EMPC design based on the subsystem models for the WWTP is described as follows:

Algorithm 3.5.1 *Implementation algorithm for distributed EMPC based on the subsystem models*

1. *At each sampling time $t_{k \geq 0}$, set $c = 1$, let the i-th EMPC controller receive subsystem state measurements $x_i(t_k)$. Let $u_i^{(0)}(\tau|t_k) = u_i^*(\tau|t_{k-1})$, and $\tilde{x}_i^{(0)}(\tau|t_k) = \tilde{x}_i^*(\tau|t_{k-1})$, where u_i^* and $\tilde{x}_i^*$ denotes the optimal input trajectory and optimal predicted state trajectory generated at time instant t_{k-1} respectively. Do the following steps:*

    1.1. *The i-th EMPC controller sends the predicted states evaluated at previous iteration $c-1$ (i.e., $\tilde{x}_i^{(c-1)}(\tau|t_k)$, $\tau \in [t_k, t_{k+N})$) and future input trajectories generated from previous iteration $c-1$ (i.e., $u_i^{(c-1)}(\tau|t_k)$, $\tau \in [t_k, t_{k+N})$) to the other controller.*

    1.2. *The i-th subsystem EMPC controller evaluates the future control input trajectory $u_i^{(c)}(\tau|t_k)$, $i = 1, 2$ and predicted state trajectories $\tilde{x}_i^{(c)}(\tau|t_k)$ based on the input and state trajectories from previous iteration (i.e., $\tilde{x}_j^{(c-1)}(\tau|t_k)$, and $u_j^{(c-1)}(\tau|t_k)$, $j \neq i$) .*

    1.3. ***If** $c = q$ **or** $|u_i^{(c)}(\tau|t_k) - u_i^{(c-1)}(\tau|t_k)| < \epsilon$, **then:***
    Let $u_i^* = u_i^{(c)}(\tau|t_k)$, and go to Step 2.
    ***Else**, do:*
    Set $c = c+1$, and go to Step 1.1.

2. *The i-th EMPC controller sends the first control input of the manipulated input $u^*(t_k|t_k)$ to the actuator.*

At time instant t_0, each EMPC controller i, $i = 1$, 2, is initialized with steady-state values of the states and the inputs of its interacting subsystems as a conservative

approximation. In step 1 of Algorithm 3.5.1, the optimal future input value $u_i^*(\tau|t_{k-1})$ for $\tau \in [t_k, t_{k+N})$ is defined with the same assumption shown in Eq. (3.11) and the corresponding predicted state $\tilde{x}_i^*(\tau|t_{k-1})$ can be then evaluated from the subsystem model for $\tau \in [t_{k+N-1}, \ t_{k+N})$.

3.5.2 Subsystem EMPC formulation

The proposed distributed EMPC based on the subsystem model is designed to optimize the economic control objective. The optimization problem for EMPC i, $i = 1, 2$ developed based on the subsystem model at time instant t_k in iteration c is formulated as follows:

$$u_i^{(c)}(\tau|t_k) = \arg \min_{u_i(\tau) \in S_i(\Delta)} \int_{t_k}^{t_{k+N}} l\left(\tilde{x}(\tau|t_k), u(\tau|t_k)\right) d\tau \tag{3.15a}$$

$$\text{s.t.} \quad \dot{\tilde{x}}_i(\tau) = f_i(\tilde{x}_i(\tau), \tilde{x}_j(\tau), u_i(\tau), u_j(\tau), p(\tau)) \tag{3.15b}$$

$$\tilde{x}_i(t_k) = x_i(t_k) \tag{3.15c}$$

$$u_j(\tau) = u_j^{(c-1)}(\tau), \quad j \neq i \tag{3.15d}$$

$$\tilde{x}_j(\tau) = \tilde{x}_j^{(c-1)}(\tau), \quad j \neq i \tag{3.15e}$$

$$u_i(\tau) \in \mathbb{U}_i \tag{3.15f}$$

$$x_i(\tau) \in \mathbb{X}_i \tag{3.15g}$$

In optimization problem Eq. (3.15), let $u_i^{(c)}(\tau|t_k)$ denotes the optimal solution to this problem. Eq. (3.15a) is the objective function of i-th EMPC controller. Eq. (3.15b) accounts for the i-th subsystem model. Eq. (3.15c) shows the predicted state value at time instant t_k is initialized with the state measurement (i.e., $x_i(t_k)$) in each iteration. Eq. (3.15d) and Eq. (3.15e) show the future input trajectory u_j and predicted state trajectory $\tilde{x}_j$ in the optimization problem of i-th controller are the value receive from last iteration $c - 1$ of j-th controller for $j \in \{1, \ 2\} \setminus \{i\}$, respectively. Eq. (3.15f) and Eq. (3.15g) are the constraints on the subsystem inputs and states. The process input is assumed to be piece-wise constant, and the optimal future input trajectory at sampling time t_{k-1} is extended by assuming $u_i^*(t|t_{k-1})$ for $t \in [t_{k+N-1}, t_{k+N})$ to be

equal to $u_i^*(t_{k+N-2}|t_{k-1})$ and the predicted state $x_i^*(\tau|t_k)$ can be calculated from the process model Eq. (3.15b).

A trajectory of u_i is achieved after the optimization problem of Eq. (3.15) is solved. The first step value of the the input sequence is applied to the process and the manipulated input of the system is defined as follows:

$$u_i(t|t_k) = u_i^*, \; t \in [t_k, t_{k+1}), \; i = 1, 2 \tag{3.16}$$

At $c = 1$, we have $u_i^{(c-1)}(\tau|t_k) = u_i^*(\tau|t_{k-1})$, and $\tilde{x}_i^{(c-1)}(\tau|t_k) = x_i^*(\tau|t_{k-1})$, for $\tau \in [t_k, t_{k+N})$. As introduced in Eq. (3.11) from Algorithm 3.4.1, the optimal future input trajectory is assumed to remain constant as its last evaluated value when the prediction time goes one sampling interval beyond the optimization window, and the predicted state value trajectory for that time period is then generated based on the subsystem model Eq. (3.15b) with the input value.

Remark 3.5.1 *If the maximum iteration number q is equal to one, the distributed EMPC design can be called as "non-iterative distributed EMPC". The implementation algorithm for non-iterative distributed EMPC may follow the same procedure with "c = 1" condition in Algorithm 3.4.1 for the design based on the entire system model and "c = 1" condition in Algorithm 3.5.1 for the design based on the subsystem model.*

Remark 3.5.2 *The WWTP is an open-loop stable process. In our distributed EMPC designs mentioned in Section 3.4 and Section 3.5, we have imposed constraints on the manipulated inputs. we have carried out extensive simulations to generate the state trajectories of the process using various manipulated input trajectories that satisfy the imposed input constraints. We found that the states of the system remain bounded in all the simulations. Therefore, the stability of the proposed DEMPC methods can be ensured due to the inherent property of the WWTP. The stability of distributed EMPC methods is a of vital importance problem and needs to be appropriately addressed. We may carry out theoretical stability analysis for distributed EMPC designs in future work.*

Remark 3.5.3 *Recursive feasibility can be ensured for the two developed distributed EMPC schemes in simulations. In this chapter, the hard constraints imposed on the system states are mild. Specifically, we require that all the system states should take non-negative values during the operation. If the initial condition is properly selected, the feasibility of our proposed distributed EMPC designs can be achieved. Moreover, we have found by carrying out extensive simulations with different settings that the recursive feasibility of the distributed EMPC design based on the centralized model is easier to achieve compared to that of the DEMPC design based on the subsystem model.*

3.6   Simulation results

In this section, the proposed control strategies introduced in Section 3.4 and Section 3.5 are applied to the BSM1 model under different weather conditions.

3.6.1   Simulation settings

The data files for the wastewater treatment process are provided by the International Water Association Website [67]. The data files contain the influent information of inlet flowrate Q_0, and the concentration Z_0 under dry, rainy and stormy weather conditions. Figure 3.3 shows the inlet flowrate under different weather conditions. The dynamic influent concentration data under dry, rain and storm conditions are shown in Figure 3.4, Figure 3.5 and Figure 3.6, respectively.

Under each weather condition, the initial condition is picked as optimal steady state value under the corresponding weather condition, respectively. Table 3.2 and Table 3.3 show the initial condition under dry weather profile in the biological reactor and the secondary settler, respectively. According to [2], the simulation time is set to be 14 days and the simulation results of last 7 days will be used to evaluate the performance index. For the three weather profiles, the main difference lies in the last 7-day period while the first 7-day information is the same. Therefore, we consider only
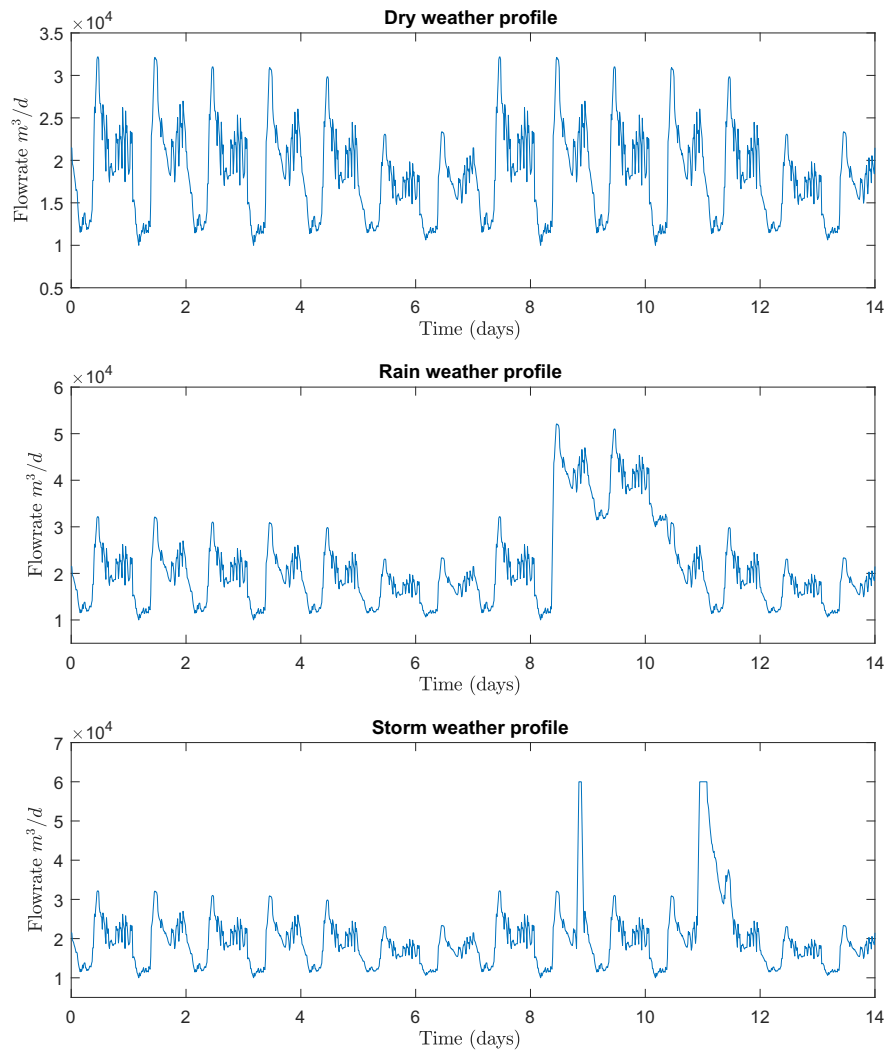
Figure 3.3: Inlet flowrate under different weather conditions
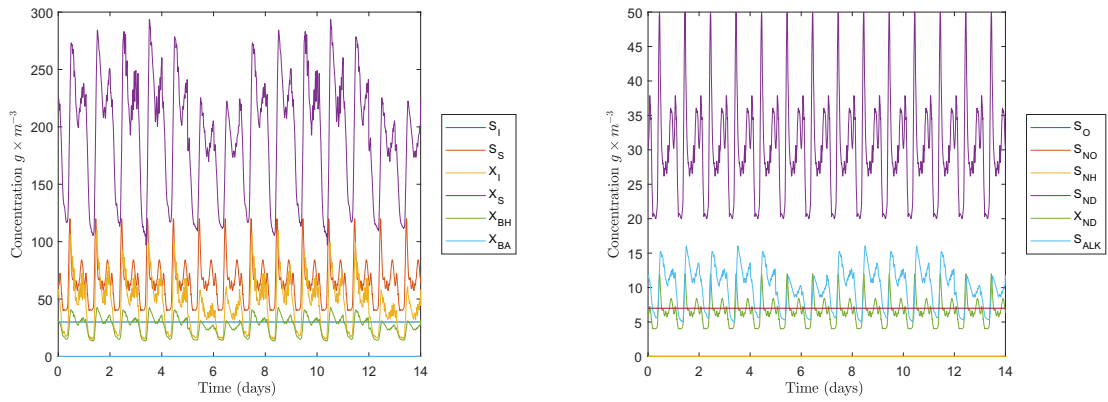
Figure 3.4: Concentration Z_0 under dry weather condition
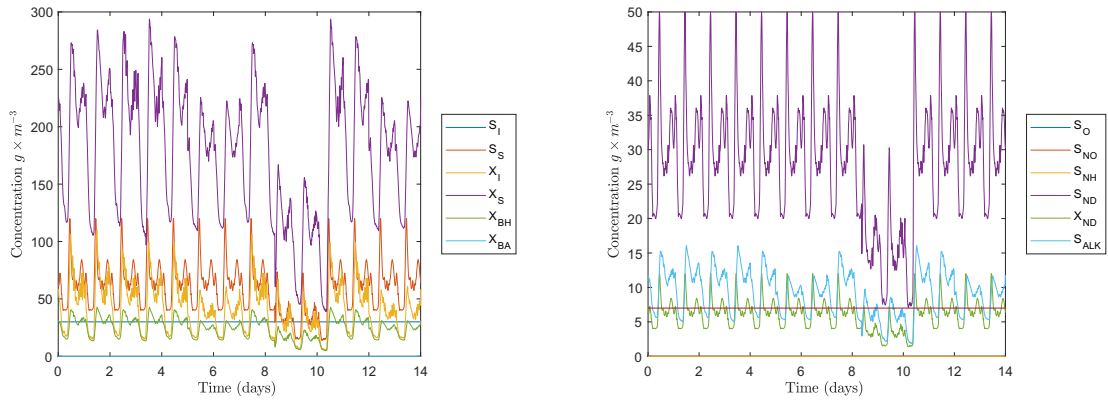
Figure 3.5: Concentration Z_0 under rain weather condition
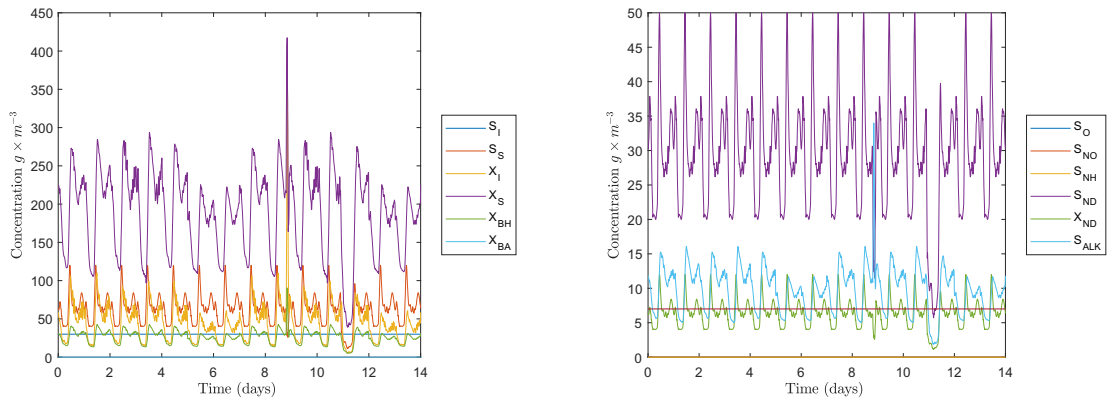
Figure 3.6: Concentration Z_0 under storm weather condition

Table 3.2: Initial conditions in biological reactor of the WWTPs in dry weather condition

Notation	Unit	Reactor 1	Reactor 2	Reactor 3	Reactor 4	Reactor 5
S_I	gCOD/m^3	30	30	30	30	30
S_s	gCOD/m^3	3.02	1.53	1.17	0.98	0.85
X_I	gCOD/m^3	1149.15	1149.15	1149.15	1149.15	1149.15
X_s	gCOD/m^3	89.42	82.27	66.48	54.73	46.83
X_{B_H}	gCOD/m^3	2551.87	2553.51	2558.79	2561.25	2561.08
X_{B_A}	gCOD/m^3	150.19	150.08	150.94	151.72	152.08
X_P	gCOD/m^3	448.05	448.94	450.13	451.31	452.50
S_O	g(-COD)/m^3	0	0	1.70	2.47	0.71
S_{NO}	gN/m^3	4.31	2.13	6.06	9.73	11.38
S_{NH}	gN/m^3	9.57	10.12	6.27	2.83	1.18
S_{ND}	gN/m^3	1.29	0.86	0.83	0.76	0.67
X_{ND}	gN/m^3	5.68	5.38	4.50	3.84	3.39
S_{ALK}	mol/m^3	5.12	5.32	4.76	4.55	4.02

Table 3.3: Initial conditions in secondary settler of the WWTPs in dry weather condition

Notation	X	S_I	S_s	S_O	S_{NO}	S_{NH}	S_{ND}	S_{ALK}
Unit	gCOD / m^3	gCOD / m^3	gCOD / m^3	g(-COD) / m^3	gN/m^3	gN/m^3	gN/m^3	mol/m^3
Layer 1	6396.71	30	0.85	0.71	11.38	1.18	0.67	4.02
Layer 2	356.18	30	0.85	0.71	11.38	1.18	0.67	4.02
Layer 3	356.18	30	0.85	0.71	11.38	1.18	0.67	4.02
Layer 4	356.18	30	0.85	0.71	11.38	1.18	0.67	4.02
Layer 5	356.18	30	0.85	0.71	11.38	1.18	0.67	4.02
Layer 6	356.18	30	0.85	0.71	11.38	1.18	0.67	4.02
Layer 7	68.99	30	0.85	0.71	11.38	1.18	0.67	4.02
Layer 8	29.54	30	0.85	0.71	11.38	1.18	0.67	4.02
Layer 9	18.12	30	0.85	0.71	11.38	1.18	0.67	4.02
Layer 10	12.50	30	0.85	0.71	11.38	1.18	0.67	4.02

the last 7-day operation when we evaluate the control performance. The sampling time of the simulation is set to be $\Delta = 15$ min. Control performance of the proposed DEMPC is investigated under different simulation settings in terms of control horizon and maximum iteration steps.

The performance of the proposed control schemes is assessed using three measures: the effluent quality level, the average economic cost and the average computation time over the full operating period. The effluent quality level assessment contains two main parts: effluent quality (EQ) and the government legislation level. For government legislation, five effluent concentrations are considered: the total nitrogen (N_{tot}) which is the sum of $S_{NO,e}$ and $S_{NKj,e}$, total suspended solid (TSS_e), ammonia ($S_{NH,e}$), chemical oxygen demand (COD_e), and biological oxygen demand (BOD_e). As introduced in [2], the flow-weighted average effluent concentrations should be within the limits shown in Table 3.4. The percentage of time the effluent concentration

Table 3.4: Effluent limits

N_{tot}	COD_e	$S_{NH,e}$	TSS_e	BOD_e
18 gNm^{-3}	100 g COD m^{-3}	4 gNm^{-3}	30 gSSm^{-3}	10 gBODm^{-3}

limits are not met must be reported.

The weighting parameters α_{EQ} and α_{OCI} in the economic index Eq. (3.9) are set to be 1 and 0.3. The weighting coefficient R in Eq. (3.13) is determined to be 0.1. The threshold value ϵ used in the termination condition in Algorithm 3.4.1 and Algorithm 3.5.1 is set to be 10^{-4}. For all control designs, the manipulated input u should be within the constraint that u_1 (i.e., internal recycle flow rate Q_a) is bounded by 0 to 5 times $Q_{0,stab}$ (18446 m^{3}day^{-1}), and the other input u_2 (i.e., oxygen transfer coefficient K_La_5) is constrained by 0 to 240 day^{-1}.

3.6.2 Results of dry weather condition

The performance of four control schemes is evaluated under dry weather condition. The four control schemes are centralized MPC, centralized EMPC, DEMPC based on the entire system model (DEMPCE), and DEMPC based on the subsystem model (DEMPCS).

The trajectories of the instantaneous effluent quality level under centralized MPC, centralized EMPC, non-iterative DEMPCE, and non-iterative DEMPCS with control horizon $N = 40$ are shown in Figure 3.7. Based on the average EQ value shown in Figure 3.7, DEMPCE shows comparable EQ value with centralized EMPC, lower EQ value than MPC, and much lower EQ value than DEMPCS. The EQ, OCI and the average economic cost are then evaluated for the four discussed control schemes with $N = 40$, and these values are shown in Table 3.5. The percentage change in terms of the average economic cost of centralized EMPC, non-iterative DEMPCS and non-iterative DEMPCE compared with centralized MPC is also shown in Table 3.5. Since the objective is to minimize the average economic cost, the smaller average economic
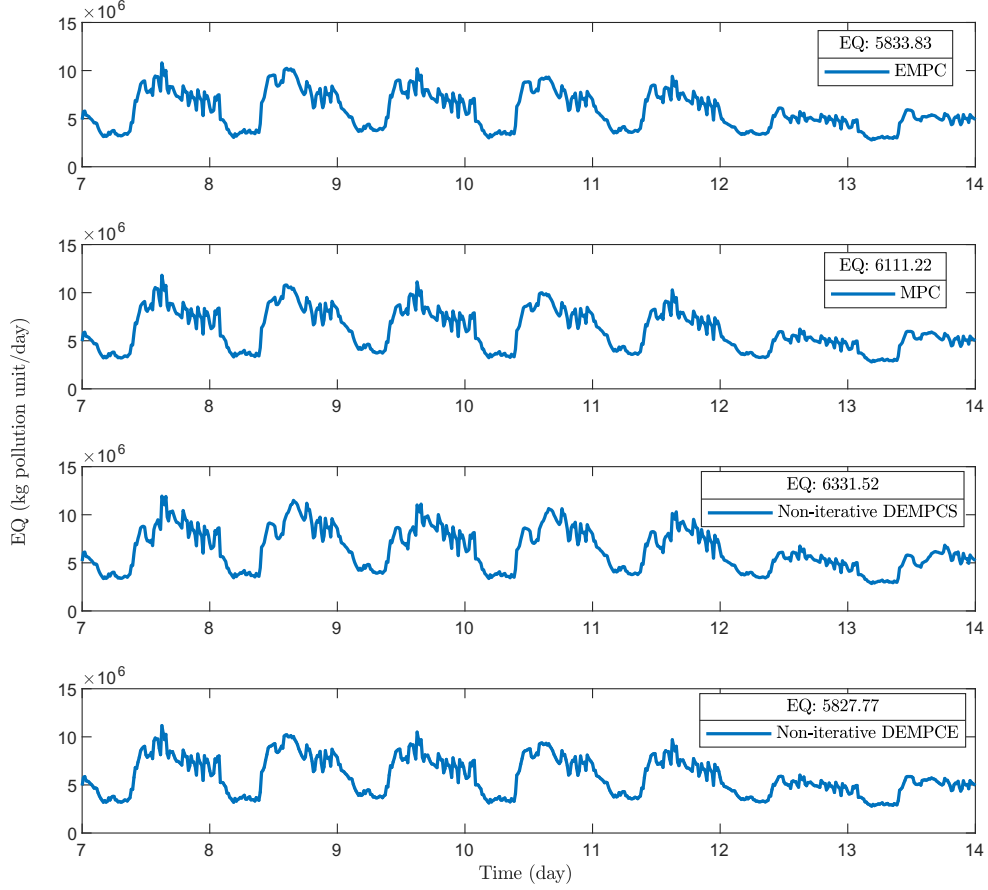
Figure 3.7: Trajectories of the instantaneous effluent quality level in dry weather condition with $N = 40$ under centralized MPC, centralized EMPC, non-iterative DEMPCE, and non-iterative DEMPCS

cost stands for better performance.

Figure 3.8 and Figure 3.9 show the trajectories of the manipulated input Q_a and $K_L a_5$ given by centralized MPC, centralized EMPC, non-iterative DEMPCE and non-iterative DEMPCS with control horizon $N = 40$, respectively. All of the manipulated inputs are within their constraints. The average computation time consumed over the full operating period is calculated based on 10 repetitive simulation runs. The average computation time over the full operating period of centralized MPC, centralized EMPC, non-iterative DEMPCS and non-iterative DEMPCE when $N = 40$
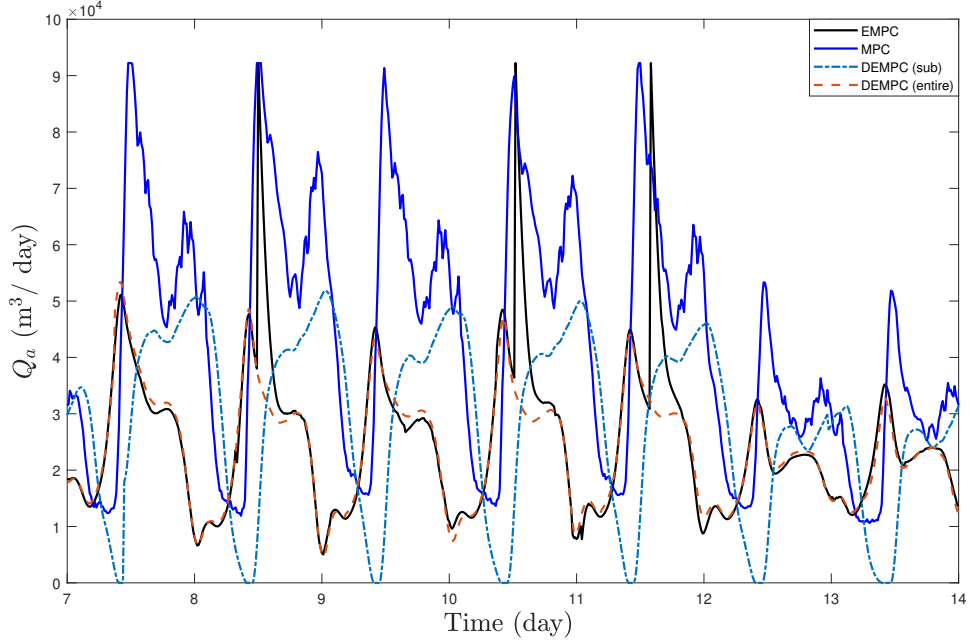
Figure 3.8: Trajectories of the manipulated input Q_a in dry weather condition with $N = 40$ under centralized MPC (blue solid line), centralized EMPC (black solid line), non-iterative DEMPCE (red dashed line), and non-iterative DEMPCS (dash dotted line)

is 6.86×10^4, 3.23×10^5, 7.94×10^4, 2.56×10^5 seconds, respectively. The average computation time consumed by the non-iterative DEMPCS is 75.42% less than centralized EMPC and 68.98% less than non-iterative DEMPCE. The main reason is that the decomposed subsystem model reduces the size of the optimization problem. We would like to note that the computational complexity of the two local controllers using the distributed EMPC design based on the subsystem model is not vastly different. Specifically, when $N = 40$, the average computation time for one-time evaluation of the controller for subsystem 1 is approximately 39.58 seconds and the average computation time for the controller of subsystem 2 is around 59.03 seconds.

Considering the government legislation, the mean value of flow-weighted average effluent concentration (i.e., N_{tot}, TSS_e, $S_{NH,e}$, COD_e, and BOD_e) under the four mentioned control schemes over the simulation time are shown in Table 3.6. The values in this table are all within the effluent limits shown in Table 3.4. Figure 3.10 shows the instantaneous effluent concentration of COD, TSS_e, and BOD_e under
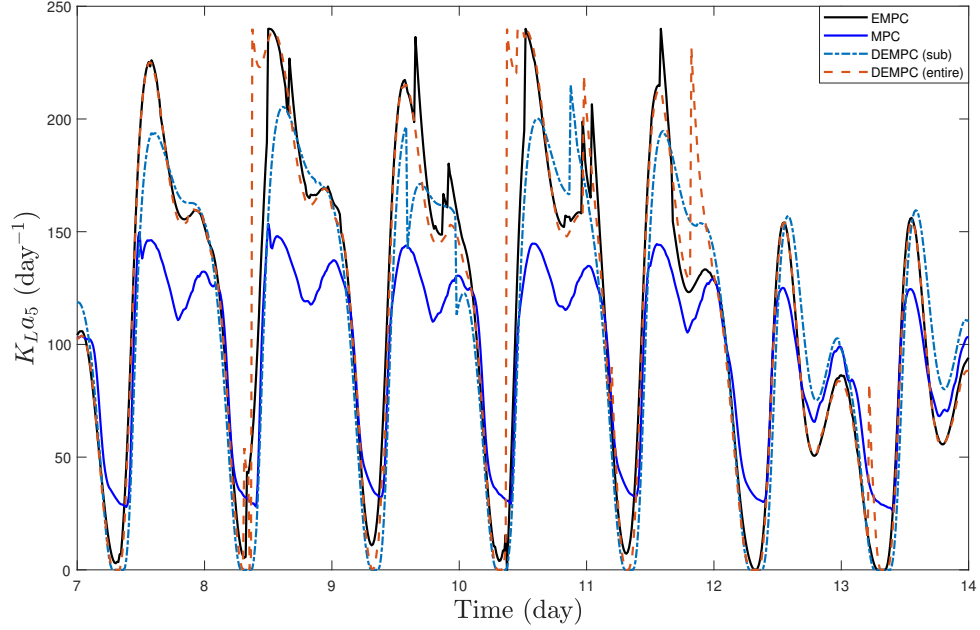
Figure 3.9: Trajectories of the manipulated input $K_L a_5$ in dry weather condition with $N = 40$ under centralized MPC (blue solid line), centralized EMPC (black solid line), non-iterative DEMPCE (red dashed line), and non-iterative DEMPCS (dash dotted line)

Table 3.5: Control performance comparison between centralized MPC, centralized EMPC, distributed EMPC based on the subsystem model (DEMPCS) and distributed EMPC based on the entire system model (DEMPCE) ($N = 40$) in dry weather condition

	Centralized MPC	Centralized EMPC	DEMPCS	DEMPCE
EQ (kg pollution /day)	6111.22	5833.83	6331.52	5827.77
OCI	16186.34	16244.14	16196.82	16697.62
Average economic cost	0.1097	0.1071	0.1119	0.1084
Percentage change compared to centralized MPC	-	-2.43%	2.00%	-1.20%

different control schemes and the concentrations are always under the limits. However, as shown in Figure 3.11, N_{tot} and SNH_e exceed the concentration limit over several time periods under the four control schemes. The effluent concentration limit is described by the solid green line in each subplot of Figure 3.10 and Figure 3.11.

The percentage of the time when the N_{tot} restriction is not satisfied is calculated to be: 5.5%, 12.0%, 7.5% and 17.4% for centralized MPC, EMPC, DEMPCE and DEMPCS, respectively. The percentage of the time when SNH_e exceeds limit is 32.24%, 14.86%, 18.87%, and 36.84% for centralized MPC, EMPC, DEMPCS and DEMPCE, respectively. We note that due to significantly fluctuating inlet flow rates, it is very challenging to fulfill the environmental regulations continuously. Feasibility issues might arise if the limits are considered in the centralized MPC, centralized EMPC and distributed EMPC designs [17].

Table 3.6: Average effluent concentration under centralized MPC, centralized EMPC, non-iterative distributed EMPC based on subsystem model and non-iterative distributed EMPC based on entire model ($N = 40$)

	Centralized MPC	Centralized EMPC	DEMPCS	DEMPCE
$\overline{N_{tot}}$ (g/m^3)	15.18	15.94	16.35	15.24
$\overline{COD_e}$ (g/m^3)	48.30	48.28	48.33	48.29
$\overline{S_{NH,e}}$ (g/m^3)	2.76	2.76	2.77	2.77
$\overline{TSS_e}$ (g/m^3)	13.03	13.04	13.04	13.03
$\overline{BOD_e}$ (g/m^3)	2.76	2.75	2.77	2.76

We also consider different sizes of the control horizon for the two DEMPC designs. Table 3.7 shows the control performance given by the two proposed schemes. The economic performance is improved for both DEMPCE and DEMPCS as N increases. The performance improvement is significant as N increases from 20 to 40. However, the performance slightly improves as N increases from 40 to 60.

Further simulations are also performed for DEMPCE and DEMPCS under $N = 60$ to investigate the influence of the terminated iteration number q. Table 3.8 shows the simulation results of DEMPCE and DEMPCS under $q = 1$ (non-iterative), $q = 3$, and $q = 5$, respectively. In terms of EQ, OCI and average economic cost, the control performance does not change too much when the terminated iteration number increases from 1 to 5 for both DEMPCE and DEMPCS. However, the average com-
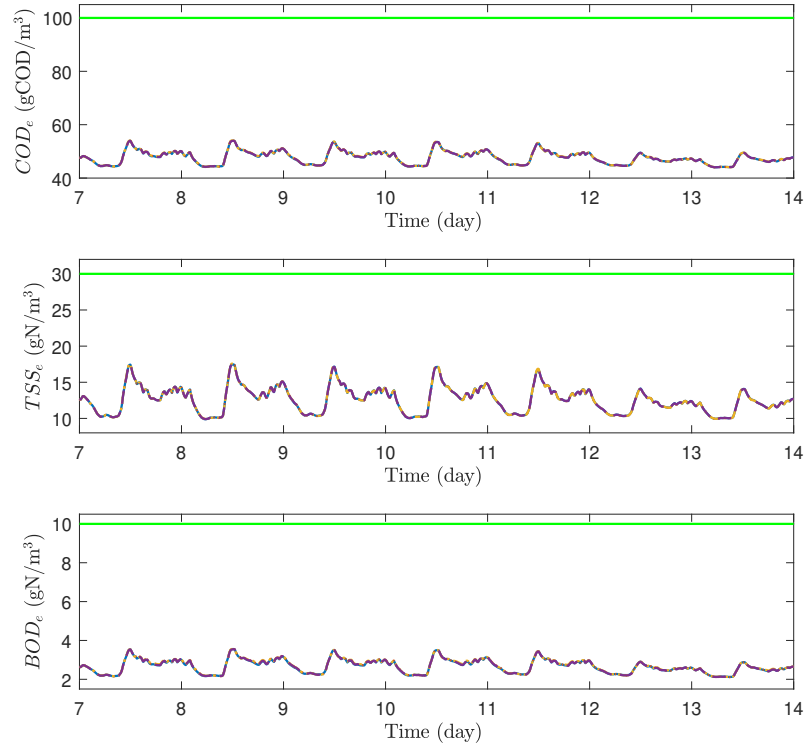
Figure 3.10: Trajectories of COD, TSS_e, and BOD_e in dry weather condition with $N = 40$ under MPC (dotted line), centralized EMPC (solid line), DEMPCE (dashed line), and DEMPCS (dash dotted line)
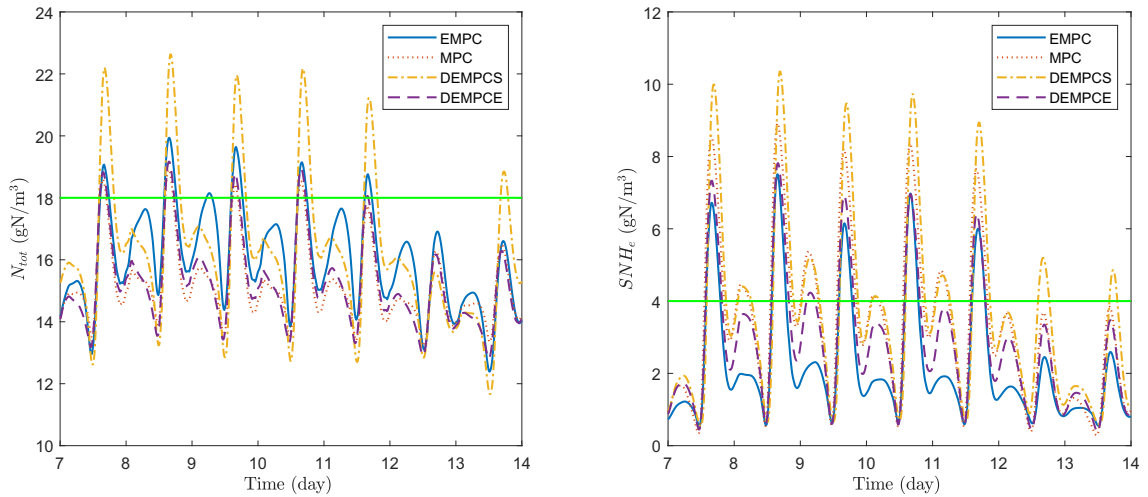
Figure 3.11: Trajectories of N_{tot} and SNH_e in dry weather condition with $N = 40$ under centralized MPC (red dotted line), centralized EMPC (blue solid line), DEMPCE (purple dashed line), and DEMPCS (yellow dashdot line)

Table 3.7: Control performance in dry weather condition under non-iterative DEMPCE and non-iterative DEMPCS with different control horizons

		EQ (kg pollution unit/day)	OCI	Average economic cost	Average computation time (s)
$N = 20$	DEMPCE	9710.17	15562.54	0.1438	1.12×10^5
	DEMPCS	6838.24	16023.11	0.1165	2.02×10^4
$N = 30$	DEMPCE	6397.11	16049.64	0.1121	1.88×10^5
	DEMPCS	6420.46	16114.70	0.1126	4.57×10^4
$N = 40$	DEMPCE	5827.77	16697.62	0.1084	2.56×10^5
	DEMPCS	6331.53	16196.83	0.1119	7.94×10^4
$N = 60$	DEMPCE	5806.45	16295.36	0.1069	5.68×10^5
	DEMPCS	6308.39	16226.32	0.1117	2.26×10^5

putation time increases significantly as the maximum iteration number q increases. Based on the consideration of computational efficiency, the non-iterative distributed EMPC designs are preferred for the wastewater treatment process.

We also investigate how the average economic cost is affected by different values of the weighting coefficient R based on DEMPCE with $N = 40$. The average economic cost equals to 0.1059, 0.1073, 0.1079, 0.1083, 0.1113 and 0.1115 when the R value equals to 0.001, 0.01, 0.05, 0.1, 0.5 and 1. Therefore, using a comparatively small weight R when penalizing the changing rate of the input for the WWTP can lead to better economic performance. In the meantime, we also find that the average computation time increases noticeably when R value decreases. We would like to improve the economic performance and reduce the computational complexity. Hence, we make a trade-off between the computational complexity and the economic performance by setting $R=0.1$ in our distributed EMPC designs.

Table 3.8: Control performance in dry weather condition under DEMPCE and DEMPCS with different iteration numbers ($N = 60$)

		EQ (kg pollution unit/day)	OCI	Average economic cost	Average computation time (s)
Non-iterative (q = 1)	DEMPCE	5806.45	16295.36	0.1069	5.68×10^5
	DEMPCS	6308.39	16226.32	0.1117	2.26×10^5
q = 3	DEMPCE	5804.32	16294.76	0.1068	1.80×10^6
	DEMPCS	6307.30	16226.07	0.1117	7.22×10^5
q = 5	DEMPCE	5804.41	16293.97	0.1068	2.89×10^6
	DEMPCS	6308.14	16223.99	0.1117	1.13×10^6

Table 3.9: Control performance comparison between centralized MPC, centralized EMPC, distributed EMPC based on the subsystem model (DEMPCS) and distributed EMPC based on the entire system model (DEMPCE) ($N = 40$) in rain weather condition

	Centralized MPC	Centralized EMPC	DEMPCS	DEMPCE
EQ (kg pollution /day)	8121.86	8010.41	8565.83	7995.05
OCI	15974.65	15969.22	15867.61	15968.70
$\overline{N_{tot}}$ (g/m^3)	13.99	14.35	15.02	14.30
$\overline{COD_e}$ (g/m^3)	52.65	52.66	52.72	52.65
$\overline{S_{NH,e}}$ (g/m^3)	3.11	2.70	3.50	2.69
$\overline{TSS_e}$ (g/m^3)	16.24	16.24	16.24	16.24
$\overline{BOD_e}$ (g/m^3)	3.47	3.47	3.49	3.47
Average economic cost	0.1291	0.1280	0.1333	0.1280
Percentage change compared to centralized MPC	-	-0.86%	3.15%	-0.86%
Average computation time (s)	8.79×10^4	3.77×10^5	8.47×10^4	3.50×10^5

3.6.3   Results of rainy and stormy weather profile

In this subsection, we also evaluate the control performance of centralized MPC, centralized EMPC, DEMPCE and DEMPCS under rainy weather and stormy weather

Table 3.10: Control performance comparison between centralized MPC, centralized EMPC, distributed EMPC based on the subsystem model (DEMPCS) and distributed EMPC based on the entire system model (DEMPCE) ($N = 40$) in storm weather condition

	Centralized MPC	Centralized EMPC	DEMPCS	DEMPCE
EQ (kg pollution /day)	7146.7	7014.54	7574.48	6979.09
OCI	17120.66	17133.14	17055.59	17169.07
$\overline{N_{tot}}$ (g/m^3)	14.66	15.22	15.80	15.40
$\overline{COD_e}$ (g/m^3)	51.46	51.46	51.52	51.45
$\overline{S_{NH,e}}$ (g/m^3)	3.29	2.69	3.73	2.52
$\overline{TSS_e}$ (g/m^3)	15.35	15.35	15.36	15.35
$\overline{BOD_e}$ (g/m^3)	3.22	3.22	3.24	3.22
Average economic cost	0.1228	0.1215	0.1269	0.1212
Percentage change compared to centralized MPC	-	-1.07%	3.23%	-1.24%
Average computation time (s)	9.15×10^4	5.00×10^5	9.68×10^4	3.89×10^5

conditions. The flow rate and the concentration of the influent flow of wastewater vary differently in rainy and stormy days compared with dry days.

Table 3.9 and Table 3.10 show the control performance of the four control schemes under rainy and stormy weather conditions. In the assessment of control performance, we consider EQ, OCI, average economic cost, the flow-weighted average effluent concentration ($\overline{N_{tot}}$, $\overline{COD_e}$, $\overline{S_{NH,e}}$, $\overline{TSS_e}$, and $\overline{BOD_e}$), and the average computation time consumed over the full operating period. The percentage change in terms of average economic cost of each control schemes compared to centralized MPC is also shown in each table. All of the average effluent concentrations are within the limitations and the instantaneous effluent concentration of N_{tot} and SNH_e sometimes may exceed the restriction value which is the same as the case under dry weather condition. From the result values in Table 3.9 and Table 3.10, DEMPCE provides comparable average economic cost with centralized EMPC, and much lower average economic

45

cost than centralized MPC. DEMPCS saves more computation time but with some control performance loss compared to other three control schemes.

3.7   Conclusions

In this chapter, distributed economic MPC (EMPC) is proposed for WWTPs described by BSM1. The WWTP is decomposed into two subsystems from the perspectives of physical topology and computational complexity. Two distributed EMPC schemes are developed. In the first design, each local EMPC controller uses a centralized model; and in the second design, each local EMPC controller uses a subsystem model. We have compared the performance of the two proposed DEMPC schemes with centralized MPC, centralized EMPC under different weather conditions. The simulation results show that the distributed EMPC based on the entire system model can achieve very similar control performance as centralized EMPC with average computation time reduced by 21%. The distributed EMPC based on the subsystem model, can improve the computation efficiency by 75% compared with the centralized EMPC. However, the control performance of the second design is degraded by approximately 5% compared with the first design where local controllers are developed based on the entire system model. The DEMPC based on the subsystem model can significantly reduce the computation load with a little degradation of control performance.

Chapter 4

Economic MPC of wastewater treatment plants based on model reduction

4.1 Introduction

In this chapter, we apply two model approximation methods to a WWTP process described by a modified nonlinear BSM1 model to overcome the intensive computation. Two computationally efficient models are obtained based on trajectory piecewise linearization (TPWL) model and reduced order TPWL model. To obtain the reduced order TPWL model, a proper orthogonal decomposition (POD) based method is utilized. Further, the reduced order model is linearized to obtain a TPWL-POD model. The objective is to design controllers which minimize the overall economic cost. Accordingly, we design EMPC controllers based on each of the models. The economic control cost can be described as a weighted summation of effluent quality (EQ) and overall operating cost (OCI). We compare the accuracy of the two proposed approximation models with different linearization point numbers. We evaluate the average computation time for the two proposed EMPC controllers and make comparisons with the EMPC based on the nonlinear model. We also investigate how the number of linearization points involved in TPWL model and TPWL-POD model affects the control performance in terms of average performance cost and the average computation
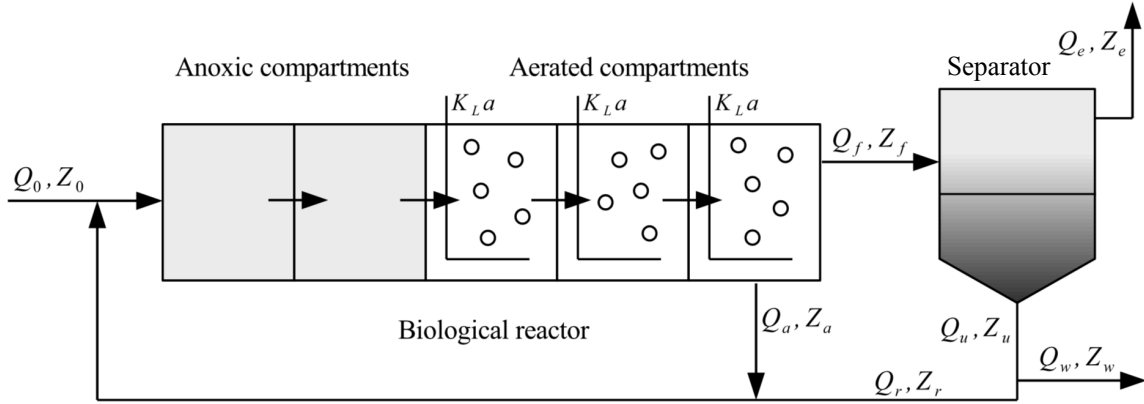
Figure 4.1: A schematic of the wastewater treatment plant

time.

4.2 Preliminaries

4.2.1 WWTP process description and modeling

The WWTP process model is based on a modified BSM1 benchmark model consisting of a five-compartment activated sludge reactor and an ideal separator. It is similar to the model described in Section 2.2, yet the secondary settler is replaced by a membrane filtration unit while the five sludge reactors remain unchanged [63]. The schematic diagram of this process is shown in Figure 4.1 [2, 63].

The dynamics of WWTP based on the modified BSM1 model can be described by 78 ordinary differential equations. The dynamics of each compartment of the reactor and the ideal separator can be described by 13 differential equations according to 13 state variables defined in Table 2.1. The parameter values of this process model are reported in [2] and Table 2.2 shows the model parameters used in this chapter. The ideal separator is assumed to be a membrane filtration unit and no biological activity exists in it [63]. All soluble compounds (i.e., S_I, S_S, S_O, S_{NO}, S_{NH}, S_{ND}, and S_{ALK}) are assumed to be well-mixed in the separator, and all solid compounds (i.e., X_I, X_S, $X_{B,H}$, $X_{B,A}$, X_P, and X_{ND}) are assumed to precipitate in the bottom of the separator [64]. Based on mass balance, the dynamics of the separator unit

$(k = 6)$ can be described as follows:

For soluble compounds in the separator unit $(k = 6)$:

$$\frac{dZ_k}{dt} = \frac{1}{V_k}(Q_f Z_f + Q_e Z_e + Q_r Z_r + Q_w Z_w) \tag{4.1}$$

$$Z_e = Z_r = Z_w = Z_k \tag{4.2}$$

$$Z_f = Z_{k-1} = Z_k \tag{4.3}$$

For solid compounds in the separator unit $(k = 6)$:

$$\frac{dZ_k}{dt} = \frac{1}{V_k}(Qf Z_f + Q_r Z_r + Q_w Z_w) \tag{4.4}$$

$$Z_r = Z_w = Z_k \tag{4.5}$$

$$Z_f = Z_{k-1} = Z_k \tag{4.6}$$

The flow rates of each stream in Figure 4.1 can be described as follows:

$$Q_1 = Q_2 = Q_3 = Q_4 = Q_5 \tag{4.7}$$

$$Q_1 = Q_a + Q_r + Q_0 \tag{4.8}$$

$$Q_f = Q_5 - Q_a = Q_e + Q_r + Q_w = Q_e + Q_u \tag{4.9}$$

$$Q_0 = Q_e + Q_w \tag{4.10}$$

4.2.2 Compact form of the system model

The modified BSM1 model for the wastewater treatment plant can be described in the following compact form:

$$\dot{x}(t) = f(x(t), u(t)) \tag{4.11}$$

where $x \in \mathbb{R}^{78}$ is the vector of process states, $u \in \mathbb{R}^3$ represents the input vector consisting manipulated inputs and the uncontrolled inputs. The manipulated inputs are the flow rate of the recirculation stream (i.e., Q_a) and the oxygen transfer rate in the fifth compartment of the biological reactor (i.e., $K_L a_5$), respectively. The uncontrolled inputs contain the influent information under different weather conditions.

4.2.3 Economic control objective

The economic control objective is defined as follows:

$$l_{eco}(x(\tau), u(\tau)) = \alpha_{EQ}\widehat{EQ}(\tau) + \alpha_{OCI}\widehat{OCI}(\tau) \tag{4.12}$$

where $\widehat{EQ}$ is the economic index effluent quality (EQ) which is calculated as the average amount of the pollutants discharged, and is defined in Eq. (3.2). $\widehat{OCI}$ represents the average amount of the economic index overall cost index (OCI) which contains the factors that affect the operating costs significantly, and it is defined in Eq. (3.7). α_{EQ} and α_{OCI} are two weighting coefficients for EQ and OCI, respectively.

4.3 Trajectory piecewise linear (TPWL) model

In this section, the trajectory piecewise linear model approach is introduced and the trajectory piecewise linear model is presented. The steps to generate the piecewise linear model are also shown in this section.

4.3.1 Piecewise Linear Representation

A linearized model for the nonlinear system can be obtained at a steady-state point (x_s, u_s) as follows:

$$\frac{dx}{dt} = f(x_s, u_s) + A(x - x_s) + B(u - u_s) \tag{4.13a}$$

$$A = \frac{\partial f}{\partial x}|_{x_s, u_s} \tag{4.13b}$$

$$B = \frac{\partial f}{\partial u}|_{x_s, u_s} \tag{4.13c}$$

where A is the Jacobian matrix of system $f(x, u)$ evaluated at the steady-state.

The simple linearized model can be used to approximate weakly nonlinear systems with less computational cost [51]. The approximated result of the linearized model usually depends on the range of inputs. If the system is a highly nonlinear system, the simple linearized model which is only linearized at one point would be less accurate.

50

The main idea of the piecewise linear model approach is to generate a weighted combination of linear models which are linearized at appropriately selected states of the original nonlinear system. Compared with the system which is linearized at one single point, the system consisting a combination of multiple linearizations would generate a better approximation result for a more complex nonlinear system.

Assuming that s linearized models have been generated for the nonlinear system Eq. (4.11) at points (x_i, u_i), $i = 0, 1, \ldots, (s-1)$:

$$\frac{dx}{dt} = f(x_i, u_i) + A_i(x - x_i) + B_i(u - u_i) \tag{4.14a}$$

$$A_i = \frac{\partial f}{\partial x}|_{x_i, u_i} \tag{4.14b}$$

$$B_i = \frac{\partial f}{\partial u}|_{x_i, u_i} \tag{4.14c}$$

A weighted combination of the linearized models in the form of Eq. (4.14) of the nonlinear system leads to the following representation:

$$\frac{dx}{dt} = \sum_{i=0}^{s-1} w_i(x)(f(x_i, u_i) + A_i(x - x_i) + B_i(u - u_i)) \tag{4.15}$$

where the weight $w_i(x)$ is a state dependent variable and it can be computed from the distance between current state x and the linearized point x_i [51].

4.3.2 Generation of piecewise linear model

The trajectory piecewise linear model is developed based on a fixed trajectory of the entire nonlinear system. The fixed trajectory is generated by simulating the nonlinear system based on a fixed training input u. Let us consider that we have generated a fixed trajectory of the nonlinear system, and the initial state x_0 is given. The selection of linearization points can be shown as follows:

Algorithm 4.3.1 *Algorithm for finding the linearization points of piecewise linear model:*

1. *Define $S = \{0, 1, \ldots, N\}$ and $S_p = \{\}$.*

2. *Set $i = 0$ and $S_l = \{x_i\}$.*

3. ***If $S \neq S_p$, then:***

   3.1. Set x_i as one of the linearization points.

   3.2. For each $j \in S \setminus S_p$,

      3.2.1 Calculate the distance between point x_j and the linearization point x_i,
      $$d_j = \|x_j - x_i\|_2.$$

      *3.2.2 **If** $d_j \leq \delta$ $(\delta > 0)$, **then**:*
      $$S_p = S_p \cup \{j\}.$$
      ***Else**, do:*
      $$S_p = S_p.$$

   3.3. Select $k_{\min}$ such that $k_{\min} = \arg\min\limits_{k} \{d_k | k \in S \setminus S_p\}$.

   3.4. Set $i = k_{min}$, set $S_l = S_l \cup \{x_i\}$. Go to Step 3.1.

   ***Else**, end.*

In the above algorithm, the "$\setminus$" denotes set subtraction such that $A \setminus B := \{x | x \in A, x \notin B\}$. N is the number of sampled points on this fixed trajectory. S_l is the set of the linearization points. The δ value is a pre-determined distance threshold, and it can be determined in the following algorithm:

Algorithm 4.3.2 *Determination of the pre-determined distance threshold δ value algorithm:*

1. *Find the maximum distance between any of the two points on the trajectory,*
   $$d_j = \|x_j - x_h\|_2, \ j, h \in \{0, 1, \ldots, N\}.$$

2. *Set $\delta = d_{max}/s$.*

In the above algorithm 4.3.2, s is the number of models supposed to be generated.

The state dependent weight $w_i(x)$ shown in Eq. (4.15) can be computed as follows [51]:

Algorithm 4.3.3 *Computation algorithm for the state dependent weight parameter* $w_i(x)$:

1. *At each linearization point* (x_i, u_i), *compute the distance* $d_i = \|x - x_i\|_2$.

2. *Find the minimum value among* d_i, $m = min_{i=0,...,(s-1)} d_i$.

3. *For* $i = 0, \ldots, (s-1)$ *compute* $\hat{w}_i = e^{-\beta d_i/m}$.

4. *Compute the summation of* $\hat{w}_i$, $S(x) = \sum_{j=0}^{s-1} \hat{w}_i(x)$.

5. *Compute the normalized parameter* $w_i(x) = \frac{\hat{w}_i(x)}{S(x)}$.

In the above approach, β is a positive constant value. The weighting parameter $w_i(x)$ changes according to the position of current state x in state space. The exponential term in step 3 to determine the weighting parameter ensures that the distribution of the weight w_i will change immediately close to one if current state x is sufficiently close to the linearization point x_i.

4.4 TPWL model based on POD method

In this section, the TPWL method is combined with the POD method to further reduce computational cost. The POD method is introduced in this section. The steps of establishing the TPWL-POD model are presented and the representation of the model is also shown in this section.

4.4.1 POD method introduction

The POD method can be used to obtain a low-order model but capture the most important dynamics of the original complicated systems [42]. POD method is a SVD-based approximation method to derive the low dimensional system to approximate the large scale system. It can be applied to both high-complexity linear and nonlinear systems [65].

Giving a fixed input u, the trajectory of state $x \in \mathbb{R}^n$ at certain time instances t_k can be measured as:

$$X = [x(t_1)\ x(t_2)\ x(t_3)\ \ldots\ x(t_N)] \tag{4.16}$$

$X \in \mathbb{R}^{n \times N}$ in (4.16) can be called as the snapshot matrix of the process data. It should be mentioned that the measured time instant points N should be much greater than the dimension of the system n, i.e., $N \gg n$. By computing the singular value decomposition of the snapshot matrix, X can be decomposed into a product of three matrices [65]:

$$X = U\Sigma V^T \in \mathbb{R}^{n \times N} \tag{4.17}$$

where $U \in \mathbb{R}^{n \times n}$ and $V \in \mathbb{R}^{N \times N}$ are orthonormal and called the left and right singular vector, respectively. $\Sigma = \mathrm{diag}(\sigma_1, \ldots, \sigma_n) \in \mathbb{R}^{n \times N}$ is a diagonal matrix, and each diagonal entry of the matrix is called the singular values. The singular values of X are nonnegative numbers and ordered in a decreasing way, i.e., $\sigma_1 \geq \sigma_2 \geq \cdots \geq \sigma_n$. The greater σ value represents the basis vector captures the more important information present in the data [66]. If the singular values of the matrix drop off rapidly, we can obtain a low-dimensional approximated system [65]:

$$X = U\Sigma V^T \approx U_k \Sigma_k V_k^T,\ \ k \ll n \tag{4.18}$$

Let $x(t) \approx U_k z(t),\ z(t) \in \mathbb{R}^k$, the reduced-order system model can be shown as follows:

$$\dot{z}(t) = U_k^T f(U_k z(t), u(t)) \tag{4.19}$$

where $z(t)$ is the approximation of states $x(t)$ in a low-dimensional space which is spanned by the first k columns of the left singular vector of X [65], i.e., U_k.

4.4.2   TPWL-POD model representation

Assuming we have generated the reduced order basis U_k via POD method for the process system, and the reduced order model of the system is with k states. The

relationship between state x with order N in the original space and projection z with order k ($k \ll N$) in reduced-order space can be represented in the following form:

$$x = U_k z \qquad (4.20)$$

where $U_k \in \mathbb{R}^{N \times k}$ is an orthogonal matrix and represents the projection of x in original space onto z in the reduced-order space.

Combining with Eq. (4.20), the TPWL model Eq. (4.15) generated in Section 4.3.1 can be represented as follows:

$$\frac{d(U_k z)}{dt} = \sum_{i=0}^{s-1} w_i(z)(f(U_k z_i, u_i) + A_i(U_k z - U_k z_i) + B_i(u - u_i)) \qquad (4.21)$$

Where z_i is the projection of the linearized points x_i in the reduced-order space, and $[z_0, z_1, \ldots, z_{s-1}] = \left[U_k^T x_0, U_k^T x_1, \ldots, U_k^T x_{s-1} \right]$

Multiplying Eq. 4.21 by U_k^T, the model can be shown as:

$$\frac{dz}{dt} = \sum_{i=0}^{s-1} w_i(z)(A_{ir} z + B_{ir} u + \gamma_{ir}) \qquad (4.22)$$

where

$$A_{ir} = U_k^T A_i U_k$$

$$B_{ir} = U_k^T B_i$$

$$\gamma_{ir} = U_k^T (f(x_i, u_i) - A_i x_i - B_i u_i)$$

$$\sum_{i=0}^{s-1} w_i(z) = 1$$

The weight $w_i(z)$ is calculated based on the distance between current projected state z and the linearization point z_i, and it follows the Algorithm 4.3.3 shown in Section 4.3.1.

4.4.3 Generation method of TPWL-POD model

The generation of the reduced order TPWL-POD model consists of two parts: generation of the POD reduced basis and the generation of trajectory piecewise linear model. Figure 4.2 shows the methodology used in this work.
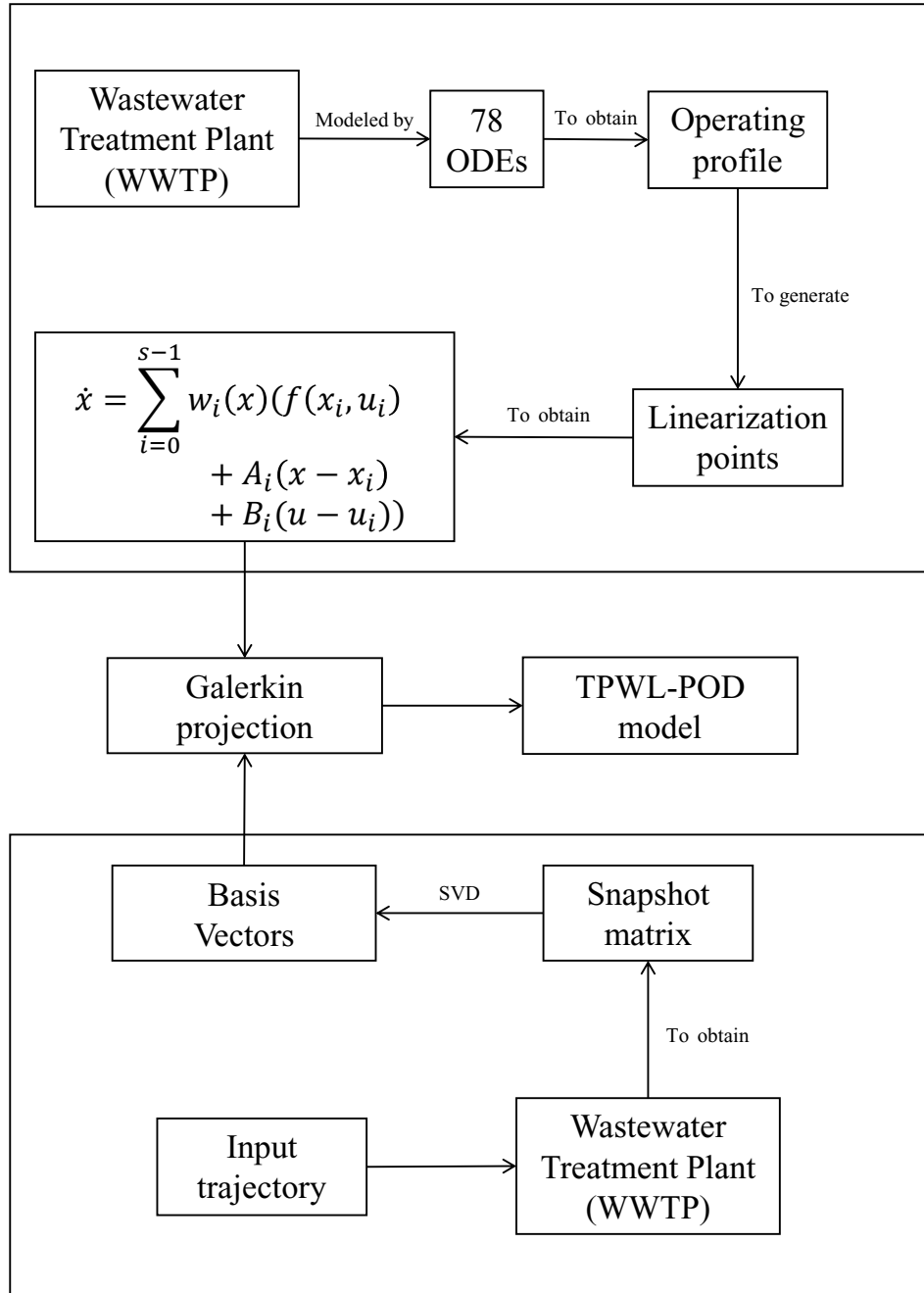
Figure 4.2: TPWL-POD framework

The strategy to generate the POD basis for WWTP process is described by the following algorithm:

Algorithm 4.4.1 *Generation of POD basis algorithm:*

1. *Simulate the nonlinear system for $t \in (0, N]$ to generate the snapshot matrix of*

the process, i.e., X.

2. *Take singular value decomposition on snapshot matrix X, $X = U\Sigma V^T$.*

3. *Determine the proper reduced order k to choose the k most relevant basis vectors of the system.*

4. *Generate the POD basis vectors matrix U_k.*

The strategy to generate the piecewise linear model is the same as the one shown in Section 4.3.2. After generating the linearization points x_i, these linearization points are projected to the reduced-order space, i.e., $z_i = U_k^T x_i$. The weighting parameter $w_i(z)$ is computed based on the states in reduced-order space, and the strategy to calculate it is the same as the steps in Algorithm 4.3.3.

4.5 Centralized EMPC design based on TPWL model and TPWL-POD model

In this section, we present the proposed centralized EMPC design based on two different models. The two considered models are as follows: TPWL model introduced in Section 4.3 and TPWL-POD model introduced in Section 4.4. The control objective is to minimize the economic cost introduced in Section 4.2.3.

4.5.1 Centralized EMPC design based on TPWL model

First, the nonlinear model of the WWTP system is linearized using the trajectory piecewise linearization method proposed in Section 4.3. The EMPC developed based on the TPWL model can be formulated as the following optimization problem:

$$u^*(\tau|t_k) = \arg\min_{u(\tau)\in S(\Delta)} \int_{t_k}^{t_{k+N}} l\left(\tilde{x}(\tau), u(\tau)\right) d\tau \qquad (4.23a)$$

$$\text{s.t.} \qquad \dot{\tilde{x}}(\tau) = \sum_{i=0}^{s-1} w_i(\tilde{x}(\tau))(f(x_i, u_i) + A_i(\tilde{x}(\tau) - x_i) + B_i(u(\tau) - u_i)) \qquad (4.23b)$$

$$\tilde{x}(t_k) = x(t_k) \tag{4.23c}$$

$$u(\tau) \in \mathbb{U} \tag{4.23d}$$

In the above optimization problem Eq. (4.23), $u^*(\tau|t_k)$ is the optimal solution to the problem. Eq. (4.23a) denotes the objective function for the centralized EMPC controller that minimizes the economic cost l defined in Eq. (4.12), N denotes the control horizon, and $S_i(\delta)$ represents a family of piecewise-constant functions. Eq. (4.23b) is the approximated piecewise linear model of the nonlinear system as introduced in Section 4.3. The state measurement value at current sampling time t_k (i.e., $x(t_k)$) is used to initialize the predicted state trajectory in Eq. (4.23c). Eq. (4.23d) is the constraint on input u.

The optimal input trajectory is achieved after the optimization problem Eq. (4.23) is solved (i.e., $u^*(\tau|t_k)$). The first step value of the input trajectory is defined to be the manipulated input applied to the operating process at time instant t_k, which can be shown as follows:

$$u(t) = u^*(t|t_k), t \in [t_k, t_{k+1}) \tag{4.24}$$

4.5.2 Centralized EMPC design based on TPWL-POD model

In this section, the centralized EMPC is designed based on the TPWL-POD model. The model is linearized using TPWL method shown in Section 4.3 and the order of the nonlinear system is reduced using POD method proposed in Section 4.4. The proposed EMPC design can be shown as follows:

$$u^*(\tau|t_k) = \arg \min_{u(\tau) \in S(\Delta)} \int_{t_k}^{t_{k+N}} l\left(U_k z(\tau), u(\tau)\right) d\tau \tag{4.25a}$$

$$\text{s.t.} \quad \dot{\tilde{z}}(\tau) = \sum_{i=0}^{s-1} w_i(z)(A_{ir} z + B_{ir} u + \gamma_{ir}) \tag{4.25b}$$

$$\tilde{z}(t_k) = U_k^T x(t_k) \tag{4.25c}$$

$$A_{ir} = U_k^T A_i U_k \tag{4.25d}$$

$$B_{ir} = U_k^T B_i \tag{4.25e}$$

$$\gamma_{ir} = U_k^T(f(x_i, u_i) - A_i x_i - B_i u_i) \qquad (4.25\text{f})$$

$$\sum_{i=0}^{s-1} w_i(z) = 1 \qquad (4.25\text{g})$$

$$u(\tau) \in \mathbb{U} \qquad (4.25\text{h})$$

In the optimization problem Eq. (4.25), let $u^*(\tau|t_k)$ accounts for the optimal solution to this problem. The objective function is Eq. (4.25a). Eq. (4.25b) denotes the order reduced linear model using TPWL-POD method introduced in Section 4.4 for the nonlinear system. A_{ir}, B_{ir}, γ_{ir}, and $w_i(z)$ in model Eq. (4.25b) are shown in Eq. (4.25d), Eq. (4.25e), Eq. (4.25f) and Eq. (4.25g), respectively. In Eq. (4.25c), the predicted state in the reduced-order space is initialized with the state measurement $x(t_k)$ and it is projected to the reduced-order space by multiplying the projection matrix U_k. Eq. (4.25h) is the input constraint. The manipulated input applied to the control process is the first step value of the optimal input trajectory, i.e., $u^*(t|t_k), t \in [t_k, t_{k+1})$.

4.6   Simulation Results

In this section, we apply the TPWL method introduced in Section 4.3 and the TPWL-POD method introduced in Section 4.4 to the WWTP. The reduced order basis and the linearization points for both TPWL model and TPWL-POD model are obtained based on a given training input signal. The approximated model accuracy for the nonlinear system with TPWL model and TPWL-POD model are discussed. We apply the proposed control strategies introduced in Section 4.5.1 and Section 4.5.2 to the modified BSM1 model. The performance of these control strategies is compared in terms of effluent quality, operating cost and computational efficiency under dry weather condition.

4.6.1 Simulation settings

The dry weather condition data file are provided in the International Water Association Web site [67]. The inlet flowrate Q_0, and the concentration Z_0 of the influent flow can be found in the data file. The wastewater treatment plant is simulated with the average value of Q_0 and Z_0 under dry weather condition to achieve the optimal steady state. We consider the optimal steady state as the initial condition for this wastewater treatment process.

To compare the performance index between different control strategies, the simulation time is set to be 14 days and the simulation results of the last 7 days will be used to evaluate the control performance index. The sampling time is picked as $\Delta = 15$ min.

The weighting parameter β in Algorithm 4.3.3 is set to be 25. The weighting coefficients α_{EQ} and α_{OCI} in the economic control objective function Eq. (4.12) are considered to be 1 and 0.3. The control horizon is determined to be 25 in all EMPC controller designs. The constraints on manipulated inputs (i.e., $\mathbb{U}$) for all control designs are considered as follows:

$$0 \leq Q_a \leq 5Q_{0,\text{stab}} \tag{4.26}$$

$$0 \leq K_L a_5 \leq 240 \text{ day}^{-1} \tag{4.27}$$

where $Q_{0,\text{stab}}$ is the average dry weather influent flow rate and is equal to 18446 m^3/day.

4.6.2 Model validation and comparison

Model validation

To verify the generated TPWL model and TPWL-POD model not only work for the inputs which are very close to the given training input but also for other inputs, the accuracy of the model is investigated under different input signals. For model validation, the number of linearization points s in both TPWL model and TPWL-POD model is set to be 9, and the reduced basis order k is set to be 35 for TPWL-POD

model.

The approximated state trajectories based on TPWL model, TPWL-POD model and the actual state trajectories based on the nonlinear system model for certain process states in the first week of the operation under the training input signal and fixed input signal are presented in Figure 4.3 and Figure 4.4, respectively. For the fixed input signal, the two manipulated inputs are fixed as $K_L a_5 = 83.9405$ d^{-1} and $Q_a = 37723.4072$ m^3/day. As can be seen from Figure 4.3 and Figure 4.4, the state trajectories almost overlap each other in all the cases. The results show that TPWL model and TPWL-POD model provide accurate models for the original nonlinear WWTP system.

Model comparison

The model approximation accuracy and computation time for TPWL method and TPWL-POD method are investigated under different number of the linearization points (s).

Figure 4.5 presents the state trajectories for certain process states using TPWL model with different number of linearization points under a given input signal in dry weather condition. Figure 4.6 shows the state trajectories for those states using TPWL-POD model with different number of linearization points under the same input signal in dry weather condition.

Table 4.1 presents the root mean square error of TPWL model and TPWL-POD model with different number of the linearization points. The result elucidates that the approximated model accuracy would increase as the number of linearization points increase for both TPWL and TPWL-POD models. As can be seen from the table, under the same linearization point number, TPWL model provides a better approximation than TPWL-POD model.

Table 4.2 shows the average computation time required for the one-sampling-time simulation of the two models with different number of the linearization points.

Figure 4.3: Trajectories of the states based on nonlinear model (blue solid lines), TPWL model (red dash-dot lines), TPWL-POD model (yellow dashed lines) under training input signal in dry weather.
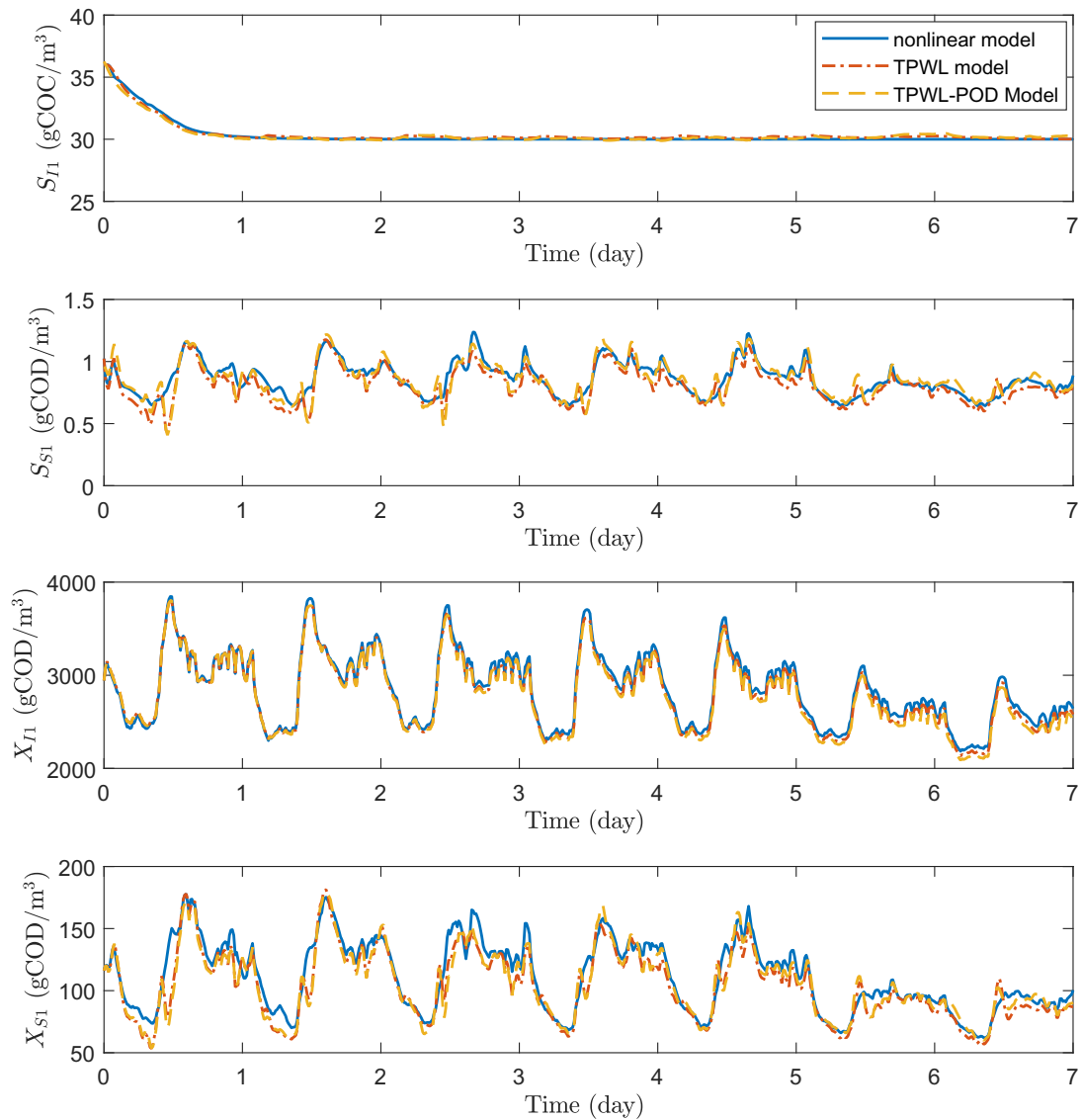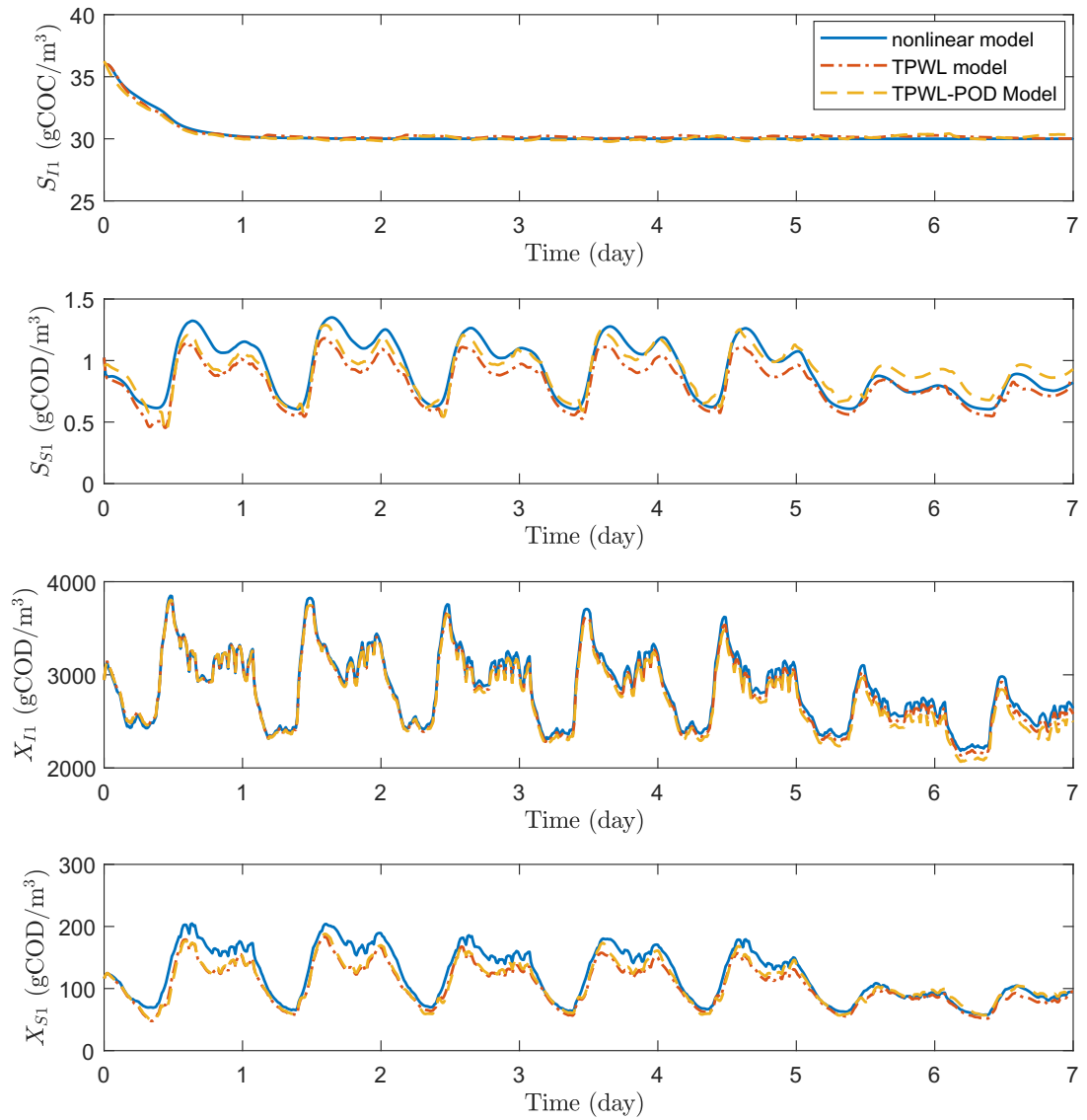
Figure 4.4: Trajectories of the states based on nonlinear model (blue solid lines), TPWL model (red dash-dot lines), TPWL-POD model (yellow dashed lines) under fixed input signal in dry weather.
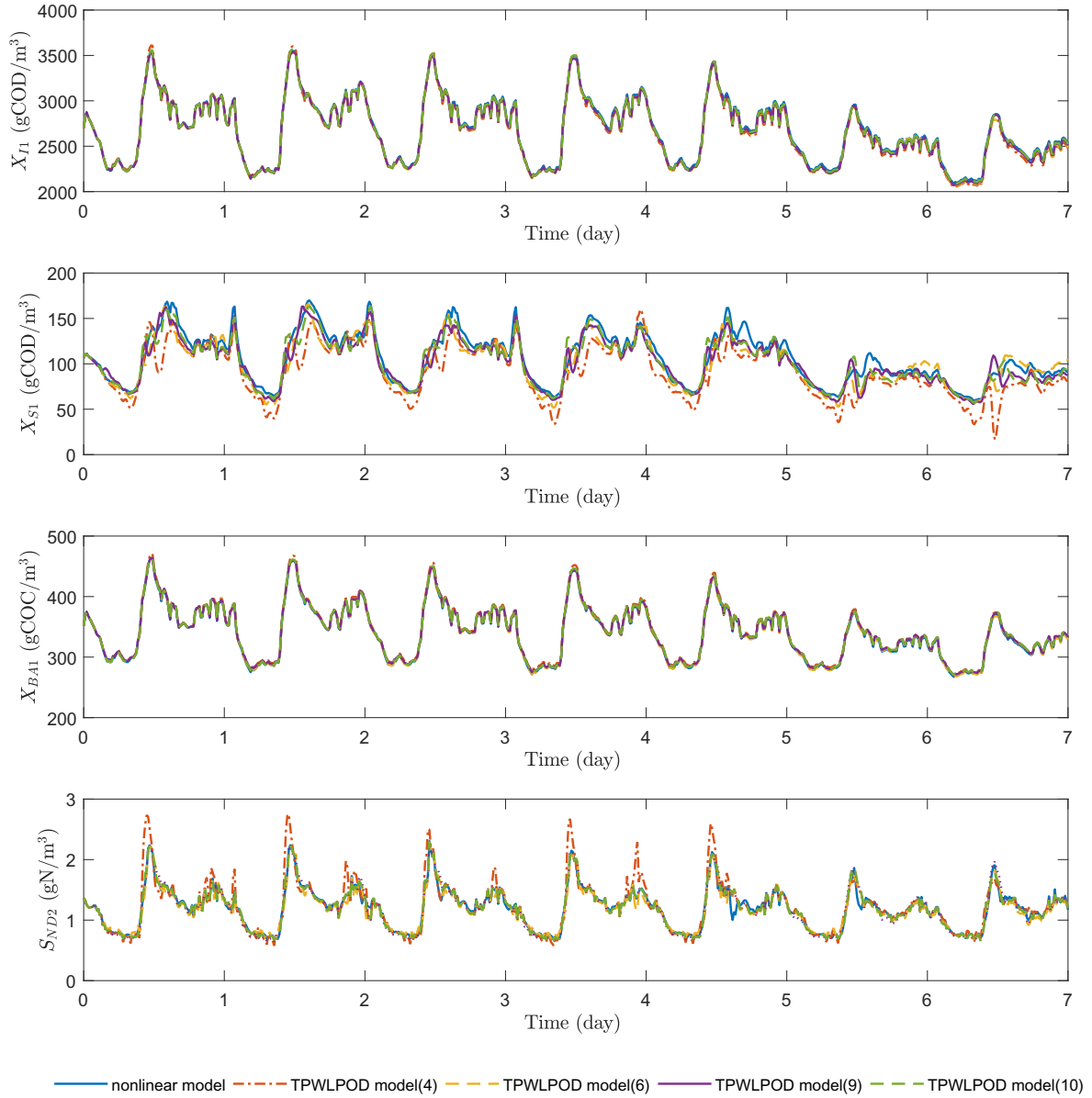
Figure 4.5: Trajectories of the states based on nonlinear model (blue solid lines), TPWL model with 4 linearization points (red dash-dot lines), TPWL model with 6 linearization points (yellow dashed lines), TPWL model with 9 linearization points (purple solid lines), and TPWL model with 10 linearization points (green dashed lines) under a given input signal in dry weather.

The result shows that the computation complexity would increase as the number of linearization points increases. Under the same linearization points number, TPWL model takes longer computation time than TPWL-POD model indicates that the
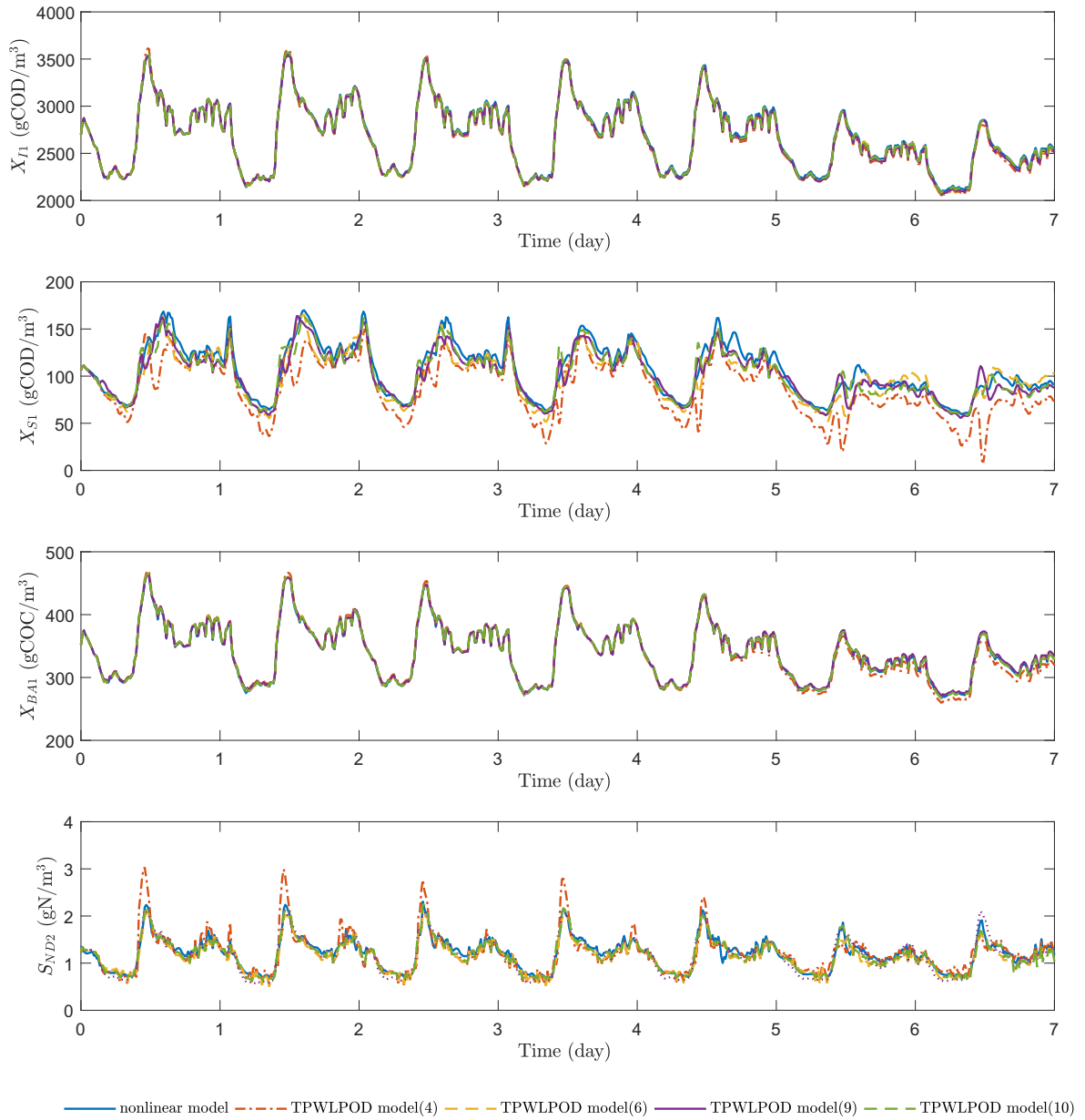
Figure 4.6: Trajectories of the states based on nonlinear model (blue solid lines), TPWL-POD model with 4 linearization points (red dash-dot lines), TPWL-POD model with 6 linearization points (yellow dashed lines), TPWL-POD model with 9 linearization points (purple solid lines), and TPWL-POD model with 10 linearization points (green dashed lines) under a given input signal in dry weather.

TPWL-POD model is more computational efficient than TPWL model.

Table 4.1: Root mean square error of TPWL model and TPWL-POD model with different number of the linearization points

Threshold δ	Linearization point number	RMSE TPWL model	RMSE TPWL-POD model
1000	4	18.3979	48.6197
950	6	10.5667	12.4511
600	9	6.0770	8.6849
570	10	5.5003	6.5913

Table 4.2: Computation time of TPWL model and TPWL-POD model with different number of the linearization points

Threshold δ	Linearization point number	Computation time (s) TPWL model	Computation time (s) TPWL-POD model
1000	4	15.000	10.31
950	6	17.408	12.01
600	9	22.404	20.13
570	10	24.095	21.18

4.6.3   Simulation results of EMPC in dry weather

We evaluate the performance of EMPC based on the nonlinear model, EMPC based on TPWL model and EMPC based on TPWL-POD model in dry weather condition, respectively.

To study the impacts of the number of linearization points (s) on EMPC design based on TPWL model, we apply the proposed EMPC scheme with $s = 4$, $s = 6$, $s = 9$, and $s = 10$ respectively. The trajectories of the instantaneous effluent quality level in dry weather condition under EMPC based on the nonlinear model, EMPC based on TPWL model with linearization point number $s = 4$, $s = 6$, $s = 9$, $s = 10$

are presented in Figure 4.7. Table 4.3 presents the calculated control performance index EQ, OCI, average economic cost, and average computation time consumed over the full operating period for EMPC based on nonlinear model and EMPC based on TPWL model with $s = 4$, $s = 6$, $s = 9$, $s = 10$. Based on the average EQ value shown in Table 4.3 and the instantaneous effluent quality level shown in Figure 4.7, we can conclude that the effluent quality level is improved as the linearization point number s in TPWL model increases. Our objective is to minimize the average economic cost. Consequently, the smaller average performance cost indicates that the model can give us a better control performance. As can be seen from Table 4.3, the EMPC with nonlinear model provides us with the best control performance, and the control performance of EMPC based on TPWL model enhances as the linearization point number raises. The EMPC based on TPWL model with $s = 4$ performs 18.24% worse than nonlinear model while the EMPC based on TPWL model with $s = 10$ is only 5.93% lower than nonlinear model. As the linearization point number s increases from 4 to 10, the control performance improves 10.42%.

To compare the computation costs for EMPC based on the nonlinear model and EMPC based on TPWL model with $s = 4$, $s = 6$, $s = 9$, $s = 10$, the average computation time consumed over the full operation period is evaluated and shown in Table 4.3. The average computation time over the full operation period is evaluated based on 10 repetitive simulation runs. The computation time consumed by EMPC based on TPWL model with $s = 4$, $s = 6$, and $s = 9$ is 30.02%, 27.97%, and 22.05% less than EMPC based on nonlinear model, respectively. However, as the linearization point number s increases, the computation load increases accordingly. The EMPC based on TPWL model with $s = 10$ is 16.29% lower than EMPC with the nonlinear model.

We also evaluate how linearization point number s influences the control performance of EMPC based on TPWL-POD model. Figure 4.8 presents the trajectories of the instantaneous effluent quality level in dry weather condition under EMPC based

Figure 4.7: Trajectories of the instantaneous effluent quality level in dry weather condition under EMPC based on nonlinear model, TPWL model with 4 linearization points, TPWL model with 6 linearization points, TPWL model with 9 linearization points and TPWL model with 10 linearization points

Table 4.3: Control performance in dry weather condition under EMPC based on nonlinear model, TPWL model with different linearization point numbers ($s = 4$, $s = 6$, $s = 9$, $s = 10$)

Model	Linearization point number	Average computation time (s)	EQ (kg pollution unit/day)	OCI	Average performance cost
Nonlinear	N/A	7.34×10^4	3896.8080	19592.3016	9774.4985
TPWL	4	5.13×10^4	5570.4105	19958.9991	11558.1102
	6	5.28×10^4	5710.0077	19404.2978	11531.2970
	9	5.72×10^4	4739.8563	19654.6556	10636.2530
	10	8.53×10^4	4349.7785	20014.8107	10354.2217

on the nonlinear model, EMPC based on TPWL-POD model with linearization point number $s = 4$, $s = 6$, $s = 9$, $s = 10$. Table 4.4 shows the EQ, OCI, average economic cost and average computation time of EMPC based on nonlinear model, EMPC based on TPWL-POD model with $s = 4$, $s = 6$, $s = 9$ and $s = 10$. We can draw the same conclusion as we have for EMPC based on TPWL model. The more linearization points we consider, the better control performance of EMPC based on TPWL-POD model would be. The average computation time consumed by TPWL-POD model will raise when the linearization point number s increases. Compared with the computation time consumed by EMPC based on the nonlinear model, EMPC based on TPWL-POD model with $s = 4$, $s = 6$, $s = 9$ and $s = 10$ is 70.13%, 67.40%, 54.51% and 15.62% less, respectively.

By examining Table 4.3 and Table 4.4, we can see that with the same linearization point number s, the computation resources used by EMPC based on TPWL-POD model is up to 58.54% less than EMPC based TPWL model used. However, the control performance of EMPC based on TPWL-POD model is around 1.39% worse than it based on TPWL model.
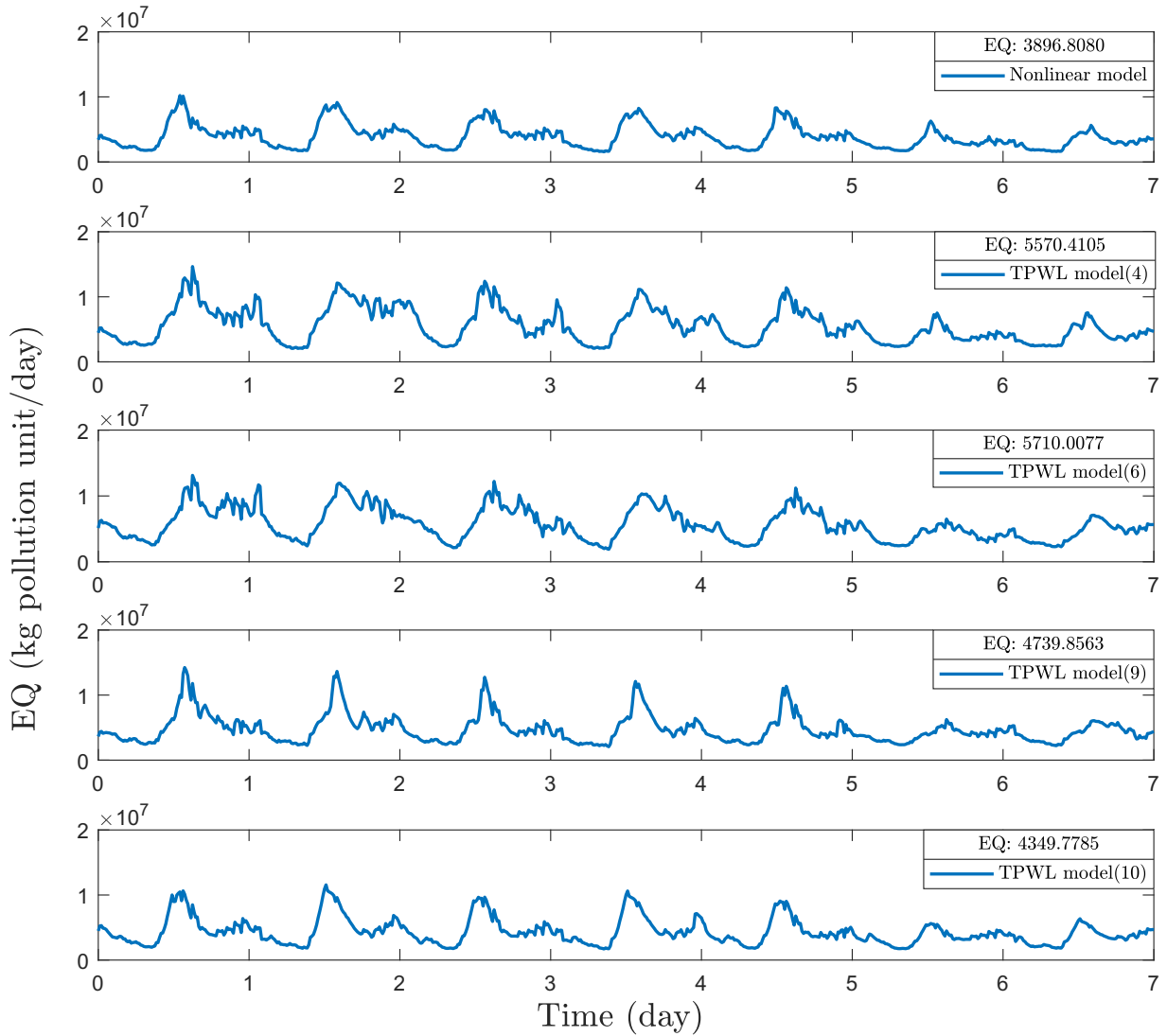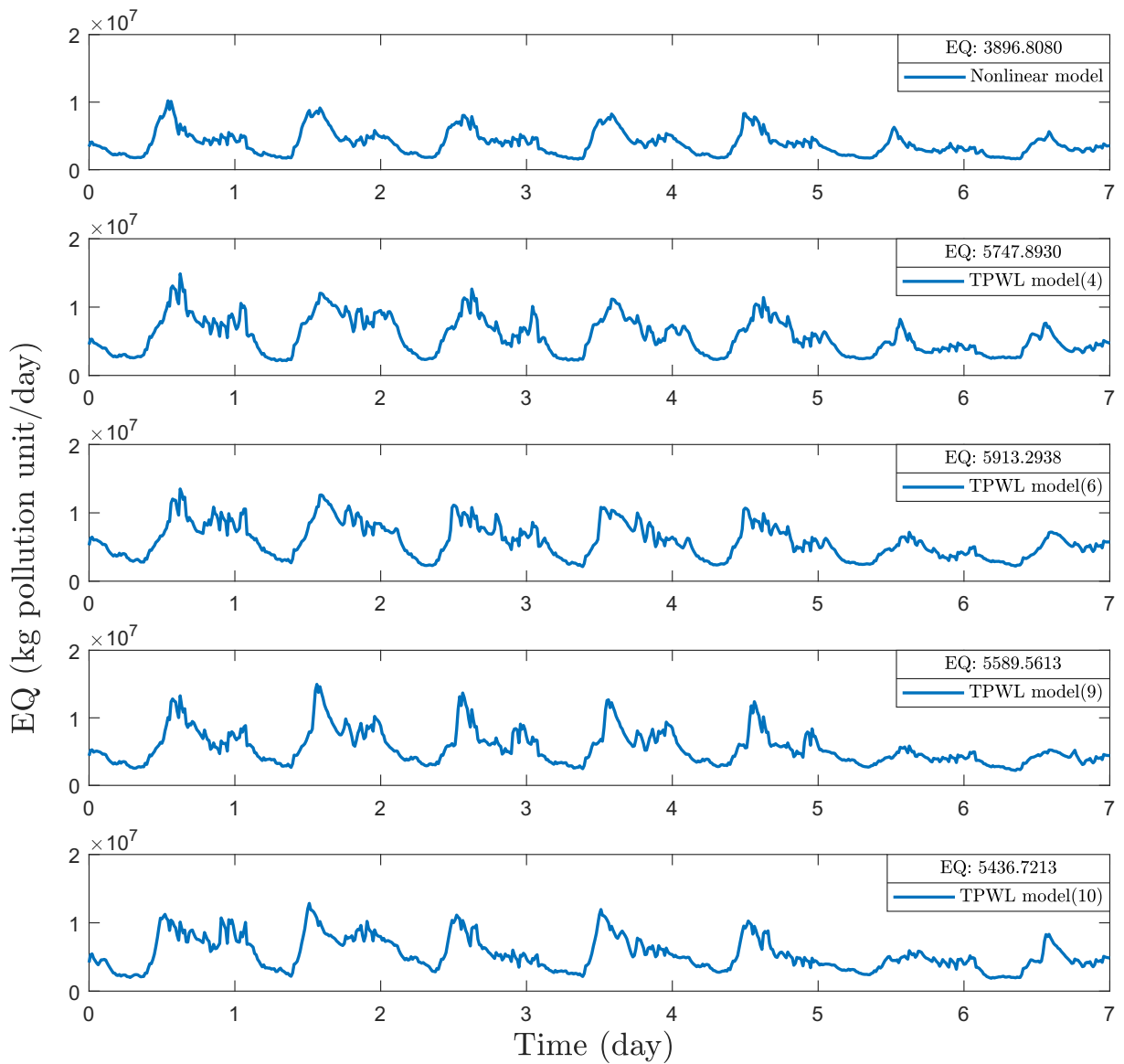
Figure 4.8: Trajectories of the instantaneous effluent quality level in dry weather condition under EMPC based on nonlinear model, TPWL-POD model with 4 linearization points, TPWL-POD model with 6 linearization points, TPWL-POD model with 9 linearization points and TPWL-POD model with 10 linearization points

Table 4.4: Control performance in dry weather condition under EMPC based on nonlinear model, TPWL-POD model with different linearization point numbers ($s = 4$, $s = 6$, $s = 9$, $s = 10$)

Model	Linearization point number	Average computation time (s)	EQ (kg pollution unit/day)	OCI	Average performance cost
Nonlinear	N/A	7.34×10^4	3896.8080	19592.3016	9774.4985
TPWL-POD	4	2.19×10^4	5747.8930	19902.6197	11718.6789
	6	2.39×10^4	5913.2938	19378.8133	11726.9378
	9	3.34×10^4	5589.5613	19328.1781	11388.0147
	10	6.19×10^4	5436.7213	19280.6409	11220.9136

4.7 Conclusions

In this chapter, two model approximation methods are applied to the modified nonlinear WWTP process. In particular, the two model approximation methods are TPWL method and TPWL-POD method. Two centralized EMPC controllers are designed based on the two models correspondingly. We have compared the model accuracy of the TPWL model and the TPWL-POD model with nonlinear model. The simulation results show that both TPWL model and TPWL-POD model can provide fairly good model accuracy. As the linearization point number s increases, the root mean square error of each model decreases. With the same linearization point number s, TPWL model provides us with a little more accurate model than TPWL-POD model while it takes much more simulation time. We have studied the relationship between linearization point number s and control performance for the two EMPC controllers. We also evaluated the computation time consumed by the two proposed EMPC controllers. The simulation results show that the control performance of the two proposed EMPC designs is improved when the linearization point number s in-

creases, while the computation efficiency degrades. With the same linearization point number s, the average computation time used by EMPC based on TPWL-POD model is up to 58.54% less than EMPC based on TPWL model. The average computation time consumed by EMPC based on TPWL-POD model is up to 70.13% lower than EMPC based on the nonlinear model. However, the control performance for EMPC based on TPWL-POD model is degraded by 1.39% compared with TPWL model and 19.89% compared with the nonlinear model.

Chapter 5

Conclusions

5.1   Summary

The objective of this thesis is to address the computational complexity problems in centralized EMPC design for wastewater treatment plants (WWTPs). The benchmark simulation model No.1 (BSM1 model) provided by the International Water Association was used to describe the dynamics of the WWTP.

In chapter 2, the descriptions of the terms and notations used in this thesis are introduced. The wastewater treatment plant model used in this thesis is described in detail in this chapter.

In chapter 3, distributed economic MPC (EMPC) is proposed for WWTPs. The WWTP is decomposed into two subsystems from the perspectives of physical topology and computational complexity. Two distributed EMPC schemes are developed. In the first design, each local EMPC controller uses a centralized model; and in the second design, each local EMPC controller uses a subsystem model. We have compared the performance of the two proposed DEMPC schemes with centralized MPC, centralized EMPC under different weather conditions. The simulation results show that the distributed EMPC based on the entire system model can achieve very similar control performance as centralized EMPC with average computation time reduced by 21%. The distributed EMPC based on the subsystem model, can improve the computation efficiency by 75% compared with the centralized EMPC. However, the control

performance of the second design is degraded by approximately 5% compared with the first design where local controllers are developed based on the entire system model. The DEMPC based on the subsystem model can significantly reduce the computation load with a little degradation of control performance.

In chapter 4, two model approximation methods are applied to our modified nonlinear WWTP process. In particular, the two model approximation methods are trajectory piecewise linearization (TPWL) method and reduced order trajectory piecewise linearization (TPWL-POD) method. Two centralized EMPC controllers are designed based on the two models correspondingly. The model accuracy, computational time, and closed-loop economic control performance under different EMPC systems are compared. The simulation results show that both TPWL model and TPWL-POD model provides a comparable model accuracy. Under the same linearization point number s, TPWL model provides us with a little more accurate model than TPWL-POD model while it takes much more simulation time. We have studied the relationship between linearization point number s and control performance for the two EMPC controllers. The control performance of the two proposed EMPC designs improves when the linearization point number s increases, while the computation efficiency degrades. We also evaluated the computation time consumed by the two proposed EMPC controllers. The simulation results show With the same linearization point number s, the average computation time used by EMPC based on TPWL-POD model is up to 58.54% less than EMPC based on TPWL model and 70.13% lower than EMPC based on the nonlinear model. However, the control performance for EMPC based on TPWL-POD model is degraded by 1.39% compared with TPWL model and 19.89% compared with the nonlinear model.

5.2 Directions for future work

In addition to the results presented in the thesis, the following research topics worth being investigated:

- The development of a distributed EMPC scheme based on the TPWL-POD model introduced in Chapter 4 to further reduce the computation cost;

- The development of output-feedback distributed EMPC for WWTP using distributed moving horizon estimation (DMHE);

- The realization of parallel computation for DEMPC and DMHE to further reduce the computation complexity.

Bibliography

[1] A. Zhang, X. Yin, S. Liu, J. Zeng, and J. Liu. Distributed economic model predictive control of wastewater treatment plants. *Chemical Engineering Research and Design*, 141:144–155, 2019.

[2] J. Alex, L. Benedetti, J. Copp, K. V. Gernaey, U. Jeppsson, I. Nopens, M. N. Pons, L. Rieger, C. Rosen, J. P. Steyer, P. Vanrolleghem, and S. Winkler. Benchmark simulation model No. 1 (BSM1). *Technical Report, Department of Industrial Electrical Engineering and Automation, Lund University*, 2008.

[3] V. C. Machado, D. Gabriel, J. Lafuente, and J. A. Baeza. Cost and effluent quality controllers design based on the relative gain array for a nutrient removal WWTP. *Water Research*, 43:5129–5141, 2009.

[4] D. Vrečko, N. Hvala, and J. Kocijan. Wastewater treatment benchmark: what can be achieved with simple control? *Water Science and Technology*, 45:127–134, 2002.

[5] R. Tzoneva. Optimal PID control of the dissolved oxygen concentration in the wastewater treatment plant. In *Proceedings of AFRICON 2007*, pages 1–7, Windhoek, South Africa, 2007.

[6] S. J. Qin and T. A. Badgwell. A survey of industrial model predictive control technology. *Control Engineering Practice*, 11:733–764, 2003.

[7] L. Fagiano and A. R. Teel. Generalized terminal state constraint for model predictive control. *Automatica*, 49:2622–2631, 2013.

[8] G. Gutierrez, L. A. Ricardez-Sandoval, H. Budman, and C. Prada. An MPC-based control structure selection approach for simultaneous process and control design. *Computers & Chemical Engineering*, 70:11–21, 2014.

[9] M. Rafiei-Shishavan, S. Mehta, and L. A. Ricardez-Sandoval. Simultaneous design and control under uncertainty: A back-off approach using power series expansions. *Computers & Chemical Engineering*, 99:66–81, 2017.

[10] B. E. Rodríguez-Pérez, A. Flores-Tlacuahuac, L. Ricardez-Sandoval, and F. J. Lozano. Optimal water quality control of sequencing batch reactors under uncertainty. *Industrial & Engineering Chemistry Research*, 57:9571–9590, 2018.

[11] M. Francisco, P. Vega, and S. Revollar. Model predictive control of BSM1 benchmark of wastewater treatment process: a tuning procedure. In *Proceedings of the 50th IEEE Conference on Decision and Control and European Control Conference (CDC-ECC)*, pages 7057–7062, Orlando, FL, USA, 2011.

[12] B. Holenda, E. Domokos, Á. Rédey, and J. Fazakas. Dissolved oxygen control of the activated sludge wastewater treatment process using model predictive control. *Computers & Chemical Engineering*, 32:1270–1278, 2008.

[13] H. G. Han, J. F. Qiao, and Q. L. Chen. Model predictive control of dissolved oxygen concentration based on a self-organizing RBF neural network. *Control Engineering Practice*, 20:465–476, 2012.

[14] W. Shen, X. Chen, and J. P. Corriou. Application of model predictive control to the BSM1 benchmark of wastewater treatment process. *Computers & Chemical Engineering*, 32:2849–2856, 2008.

[15] G. S. Ostace, V. M. Cristea, and P. Ş. Agachi. Cost reduction of the wastewater treatment plant operation by MPC based on modified ASM1 with two-step ni-

trification/denitrification model. *Computers & Chemical Engineering*, 35:2469–2479, 2011.

[16] M. O'Brien, J. Mack, B. Lennox, D. Lovett, and A. Wall. Model predictive control of an activated sludge process: A case study. *Control Engineering Practice*, 19:54–61, 2011.

[17] J. Zeng and J. Liu. Economic model predictive control of wastewater treatment processes. *Industrial & Engineering Chemistry Research*, 54:5710–5721, 2015.

[18] P. D. Christofides, R. Scattolini, D. Muñoz de la Peña, and J. Liu. Distributed model predictive control: A tutorial review and future research directions. *Computers & Chemical Engineering*, 51:21–41, 2013.

[19] R. Scattolini. Architectures for distributed and hierarchical model predictive control - A review. *Journal of Process Control*, 19:723–731, 2009.

[20] D. Jia and B. H. Krogh. Distributed model predictive control. In *Proceedings of the American Control Conference*, pages 2767–2772, Arlington, VA, USA, 2001.

[21] P. Daoutidis, M. Zachar, and S. S. Jogwar. Sustainability and process control: A survey and perspective. *Journal of Process Control*, 44:184–206, 1 2016.

[22] X. Yin, J. Zeng and J. Liu. Forming distributed state estimation network from decentralized estimators. *IEEE Transactions on Control Systems Technology*, in press. doi: 10.1109/TCST.2018.2866556.

[23] X. Yin and J. Liu. Distributed moving horizon state estimation of two-time-scale nonlinear systems. *Automatica*, 79:152–161, 1 2017.

[24] J. Liu, D. Muñoz de la Peña, and P. D. Christofides. Distributed model predictive control of nonlinear process systems. *AIChE Journal*, 55(5):1171-1184, 2009.

[25] L. Zhang, J. Wang, C. Liu. Distributed model predictive control for polytopic uncertain systems subject to actuator saturation. *Journal of Process Control*, 23(8):1075-1089, 2013.

[26] W. B. Dunbar. Distributed receding horizon control of dynamically coupled nonlinear systems. *IEEE Trans Automatic Control*, 52(7):1249-1263, 2007.

[27] L. Zhang, W. Xie, J. Wang. Robust distributed model predictive control of linear systems with structured time-varying uncertainties. *International Journal of Control*, 90(11):2449-2460, 2017.

[28] X. Chen, M. Heidarinejad, J. Liu, and P. D. Christofides. Distributed economic MPC: Application to a nonlinear chemical process network. *Journal of Process Control*, 22:689–699, 2012.

[29] J. Lee and D. Angeli. Distributed cooperative nonlinear economic MPC. In *Proceedings of the 20th International Symposium on Mathematical Theory of Networks and Systems*, pages 1-8, Melbourne, Australia, 2012.

[30] T. L. Anderson, M. Ellis, and P. D. Christofides. Distributed economic model predictive control of a catalytic reactor: Evaluation of sequential and iterative architectures. *Proceedings of IFAC International Symposium on Advanced Control of Chemical Processes*, 48:26–31, Whistler, Canada, 2015.

[31] F. Albalawi, H. Durand, and P. D. Christofides. Distributed economic model predictive control for operational safety of nonlinear processes. *AIChE Journal*, 63:3404–3418, 2017.

[32] M. A. Müller and F. Allgöwer. Distributed economic MPC: A framework for cooperative control problems. In *Proceedings of the 19th IFAC World Congress*, pages 1029–1034, Cape Town, South Africa, 2014.

[33] V. Nevistić and M. Morari. Constrained control of feedback-linearizable systems. In *Proc. 3rd European Control Conference ECC95*, pages 1726–1731, 1995.

[34] C. E. Garcia. Quadratic dynamic matrix control of nonlinear processes. An application to a batch reactor process. In *AIChE annual meeting*, 1984.

[35] G. Gattu and E. Zafiriou. Nonlinear quadratic dynamic matrix control with state estimation. *Industrial & Engineering Chemistry Research*, 31(4):1096–1104, April 1992.

[36] J. H. Lee and N. L. Ricker. Extended Kalman Filter Based Nonlinear Model Predictive Control. *Industrial & Engineering Chemistry Research*, 33(6):1530–1541, June 1994.

[37] S. L. De Oliveira. *Model predictive control (MPC) for constrained nonlinear systems.* PhD diss., California Institute of Technology, 1996.

[38] V. Nevistić. *Constrained control of nonlinear systems.* PhD diss., ETH Zurich, 1997.

[39] A. Zheng. A computationally efficient nonlinear MPC algorithm. In *Proceedings of the American Control Conference*, pages 1623–1627, Albuquerque, NM, USA, 1997.

[40] A. Zheng. Nonlinear model predictive control of the Tennessee Eastman process. In *Proceedings of the 1998 American Control Conference*, pages 1700–1704, Philadelphia, PA, USA, 1998.

[41] W. Xie, I. Bonis, and C. Theodoropoulos. Off-line model reduction for on-line linear MPC of nonlinear large-scale distributed systems. *Computers & Chemical Engineering*, 35(5):750–757, May 2011.

[42] A. Marquez, J. J. Oviedo, and D. Odloak. Model Reduction Using Proper Orthogonal Decomposition and Predictive Control of Distributed Reactor System. *Journal of Control Science and Engineering*, 2013:1–19, 2013.

[43] F. Leibfritz and S. Volkwein. Reduced order output feedback control design for PDE systems using proper orthogonal decomposition and nonlinear semidefinite programming. *Linear Algebra and its Applications*, 415(2-3):542–575, June 2006.

[44] D. Hömberg and S. Volkwein. Control of laser surface hardening by a reduced-order approach using proper orthogonal decomposition. *Mathematical and Computer Modelling*, 38(10):1003–1028, November 2003.

[45] H. V. Ly and H. T. Tran. Modeling and control of physical processes using proper orthogonal decomposition. *Mathematical and computer modelling*, 33(1-3):223–236.

[46] J. A. Atwell and B. B. King. Proper orthogonal decomposition for reduced basis feedback controllers for parabolic equations. *Mathematical and Computer Modelling*, 33(1-3):1–19, January 2001.

[47] R. Padhi and S. N. Balakrishnan. Proper orthogonal decomposition based optimal neurocontrol synthesis of a chemical reactor process using approximate dynamic programming. *Neural Networks*, 16(5-6):719–728, June 2003.

[48] X. Yin and J. Liu. State estimation of wastewater treatment plants based on model approximation. *Computers & Chemical Engineering*, 111:79–91, 2018.

[49] L. Lao, M. Ellis, and P. D. Christofides. Economic model predictive control of parabolic PDE systems: Addressing state estimation and computational efficiency. *Journal of Process Control*, 24(4):448–462, April 2014.

[50] L. Lao, M. Ellis, and P. D. Christofides. Economic Model Predictive Control of Transport-Reaction Processes. *Industrial & Engineering Chemistry Research*, 53(18):7382–7396, May 2014.

[51] M. Rewienski and J. White. A trajectory piecewise-linear approach to model order reduction and fast simulation of nonlinear circuits and micromachined devices. *IEEE Transactions on Computer-Aided Design of Integrated Circuits and Systems*, 22(2):155–170, February 2003.

[52] M. Henze, C. P. L. Grady, W. Gujer, G. V. R. Marais, and T. Matsuo. A general model for single-sludge wastewater treatment systems. *Water Research*, 21(5):505–515, May 1987.

[53] I. Takács, G. G. Patry, and D. Nolasco. A dynamic model of the clarification-thickening process. *Water Research*, 25:1263–1271, 1991.

[54] P. A. Vanrolleghem, U. Jeppsson, J. Carstensen, B. Carlssont, and G. Olsson. Integration of wastewater treatment plant design and operation - a systematic approach using cost functions. *Water Science and Technology*, 34:159–171, 1996.

[55] X. Yin, B. Decardi-Nelson, and J. Liu. Subsystem decomposition and distributed moving horizon estimation of wastewater treatment plants. *Chemical Engineering Research and Design*, 134:405–419, 2018.

[56] X. Yin and J. Liu. Subsystem decomposition of process networks for simultaneous distributed state estimation and control. *AIChE Journal*, 65(3):904–914, 2019.

[57] D. Pourkargar, A. Almansoori, and P. Daoutidis. Comprehensive study of decomposition effects on distributed output tracking of an integrated process over a wide operating range. *Chemical Engineering Research and Design*, 134:553–563, 2018.

[58] W. Tang and P. Daoutidis. Network decomposition for distributed control through community detection in inputoutput bipartite graphs. *Journal of Process Control*, 64:7–14, 2018.

[59] S. S. Jogwar and P. Daoutidis. Community-based synthesis of distributed control architectures for integrated process networks. *Chemical Engineering Science*, 172:434–443, 2017.

[60] D. Pourkargar, A. Almansoori, and P. Daoutidis. Impact of decomposition on distributed model predictive control: A process network case study. *Industrial & Engineering Chemistry Research*, 56:9606–9616, 2017.

[61] P. Daoutidis, W. Tang, and S. S. Jogwar. Decomposing complex plants for distributed control: Perspectives from network theory. *Computer & Chemical Engineering*, 114:43–51, 2018.

[62] X. Yin K. Arulmaran, J. Liu, and J. Zeng. Subsystem decomposition and configuration for distributed state estimation. *AIChE Journal*, 62:1995–2003, 2016.

[63] J. Busch, D. Elixmann, P. Kühl, C. Gerkens, J. P. Schlöder, H. G. Bock, and W. Marquardt. State estimation for large-scale wastewater treatment plants. *Water Research*, 47(13):4774–4787, September 2013.

[64] J. Zeng, J. Liu, T. Zou, and D. Yuan. State estimation of wastewater treatment processes using distributed extended Kalman filters. In *2016 IEEE 55th Conference on Decision and Control (CDC)*, pages 6721–6726, Las Vegas, NV, USA, December 2016.

[65] A. C. Antoulas. Approximation of Large-Scale Dynamical Systems: An Overview. *IFAC Proceedings Volumes*, 37(11):19–28, July 2004.

[66] A. Chatterjee. An introduction to the proper orthogonal decomposition. *Current Science*, 78(7):808–817, 2000.

[67] International Water Association. http://www.benchmarkwwtp.org.